Inverse problems in cardiovascular continuum mechanics and medical applications

Prof. Stéphane AVRIL

MINES SAINT-ETIENNE
First Grande Ecole
outside Paris
Founded in 1816

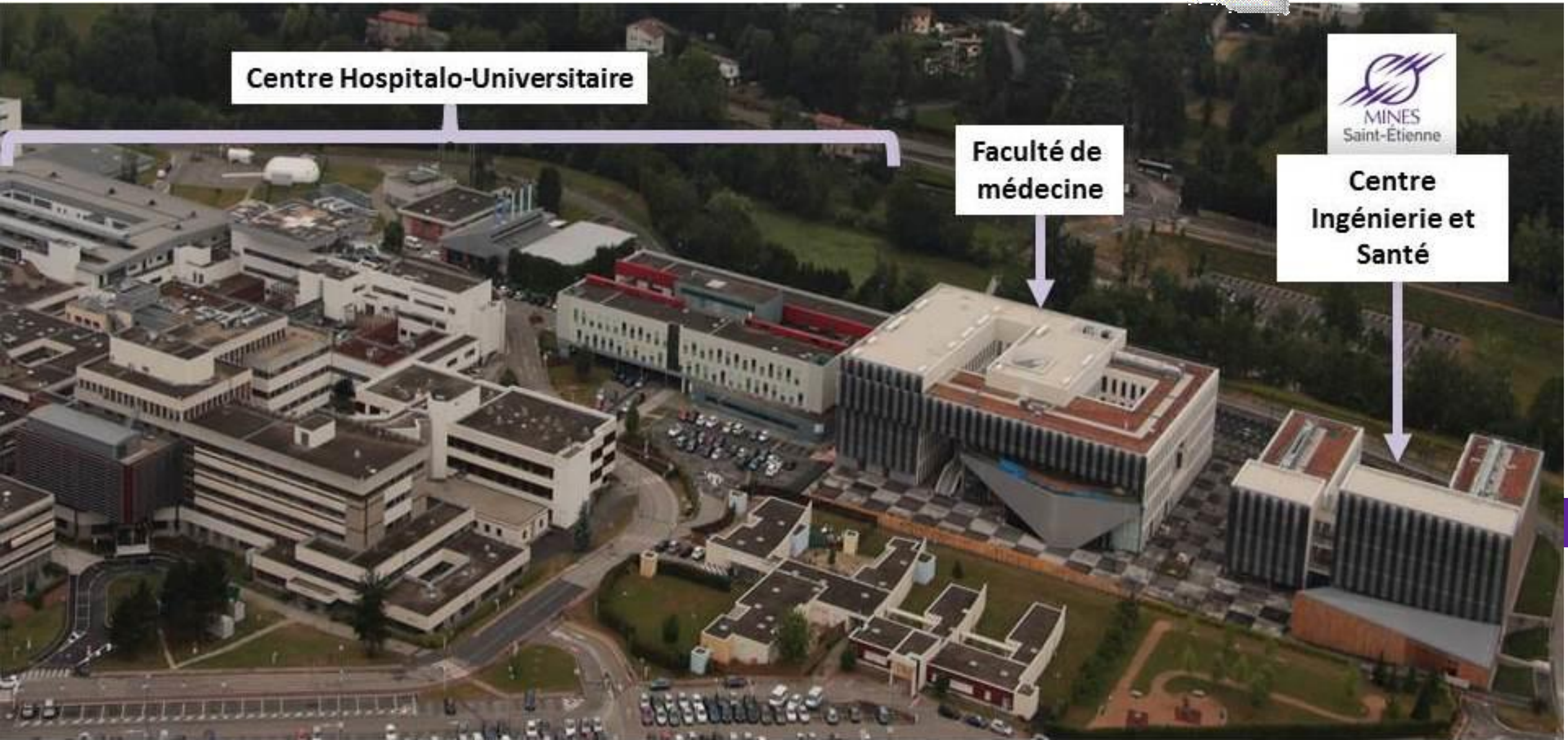

Prediction of risk of rupture and dissection

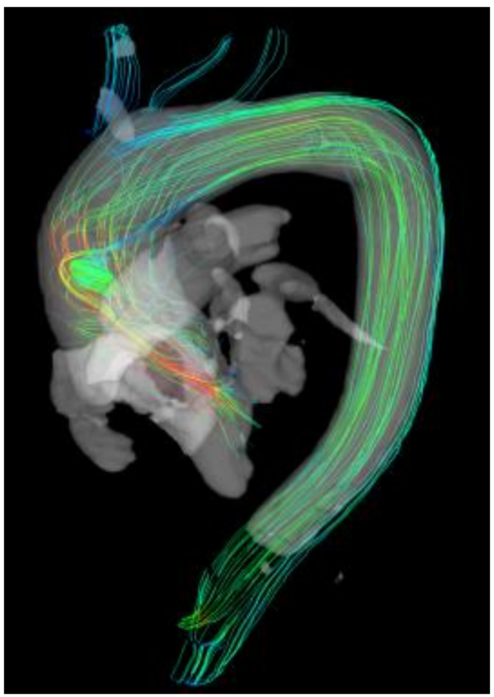

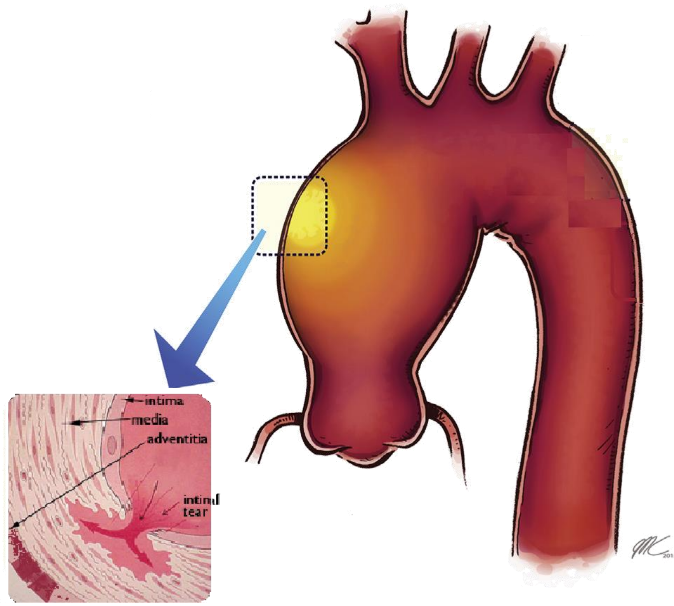

dissection

avril@emse.fr

MINES Saint-Étienne

Basics of arterial mechanics

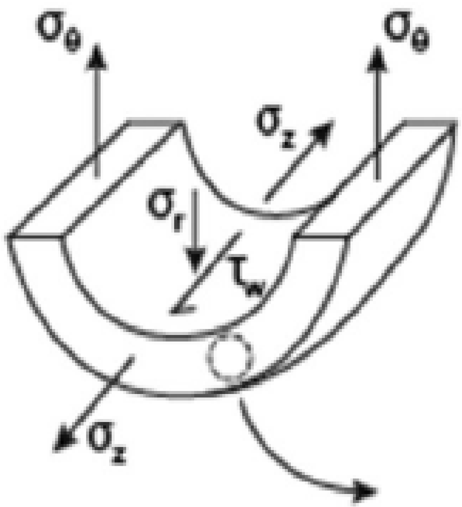

$$\tau_w = \frac{4\mu Q}{\pi a^3}, \qquad \sigma_\theta = \frac{Pa}{h}$$

Humphrey JD (2002) *Cardiovascular Solid Mechanics: Cells, Tissues, and Organs*, Springer-Verlag, NY

"we see that the greatest need lies in the direction of collecting data in multiaxial loading conditions and formulating a theory for the general rheological behavior of living tissues when stresses and strains vary with time in an arbitrary manner."

Y.C. Fung (1973)

MINES Saint-Étienne

Collection of the samples

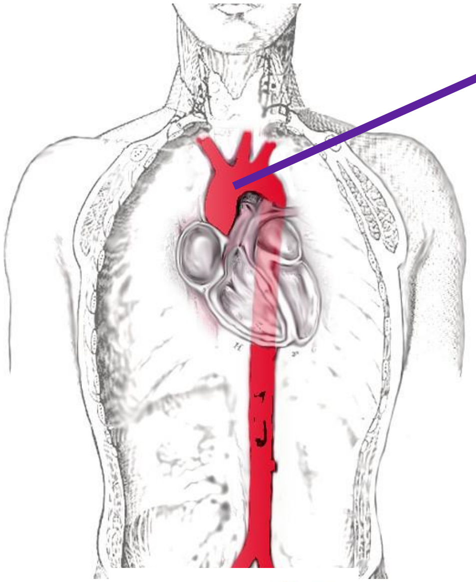

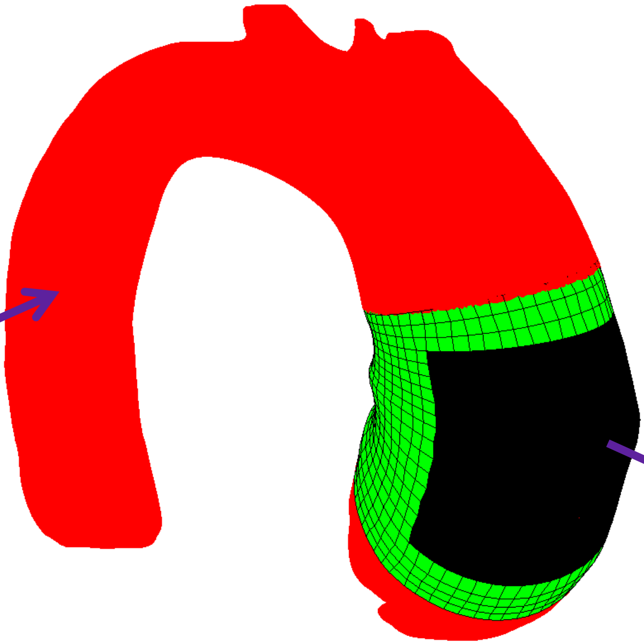

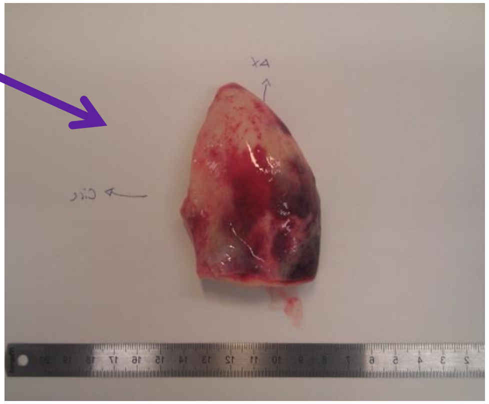

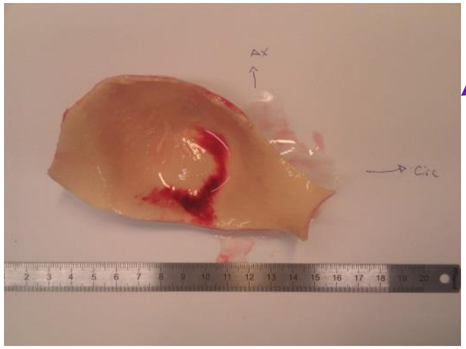

Preparation

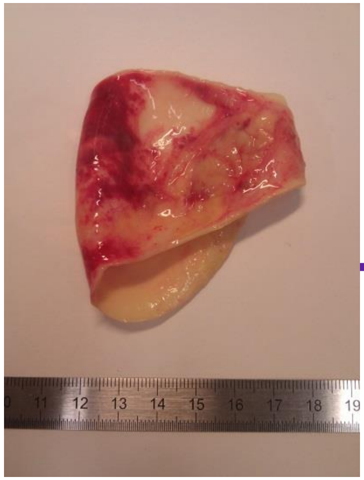

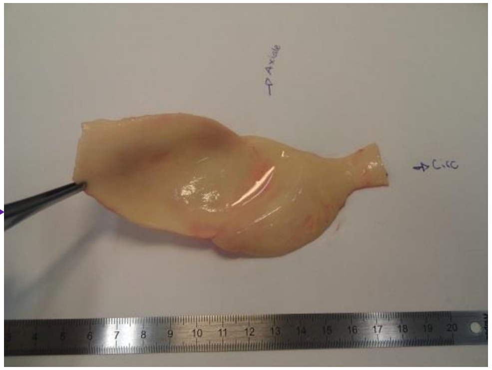

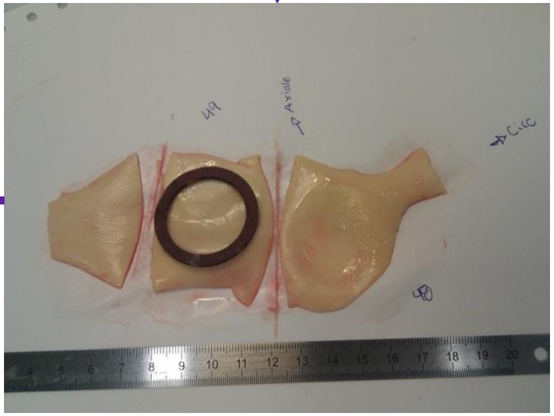

avril@emse.fr

MINES Saint-Étienne

Material characterization and constitutive modeling

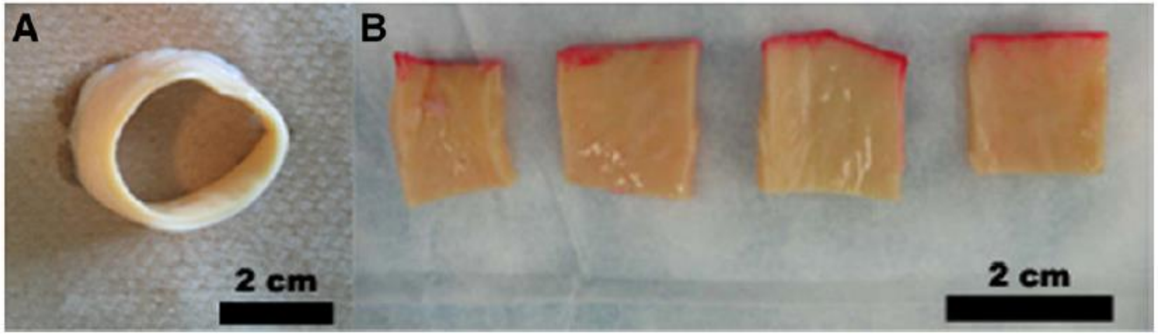

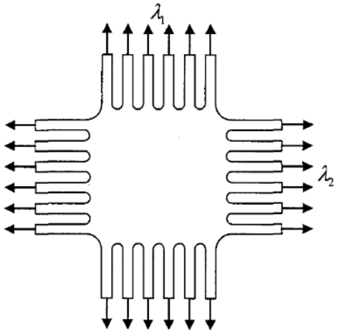

$$W = C_{10}\left(\bar{I}_1 - 3\right) + \frac{1}{D}\left(\frac{J^2 - 1}{2} - \ln J\right)$$
$$+ \frac{k_1}{2k_2}\sum_{\alpha=1}^{N}\left\{\exp\left[k_2\left\langle \bar{E}_\alpha\right\rangle^2\right] - 1\right\}$$

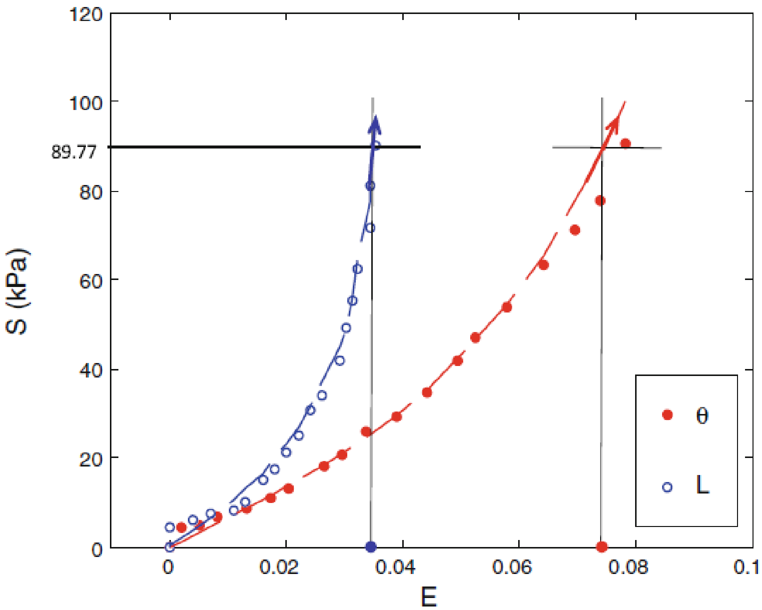

Bulge inflation test

Romo et al. Journal of Biomechanics -2014.

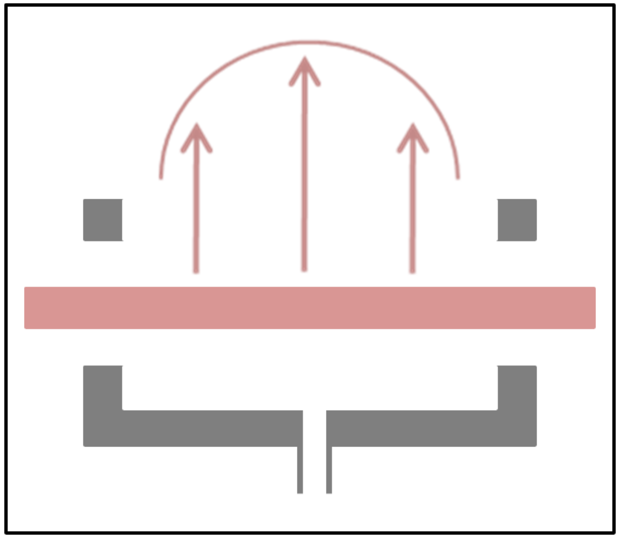

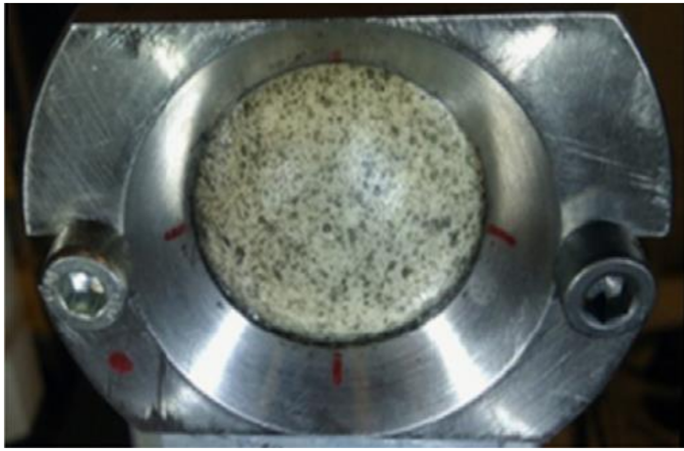

avril@emse.fr

Full-field measurements using sDIC

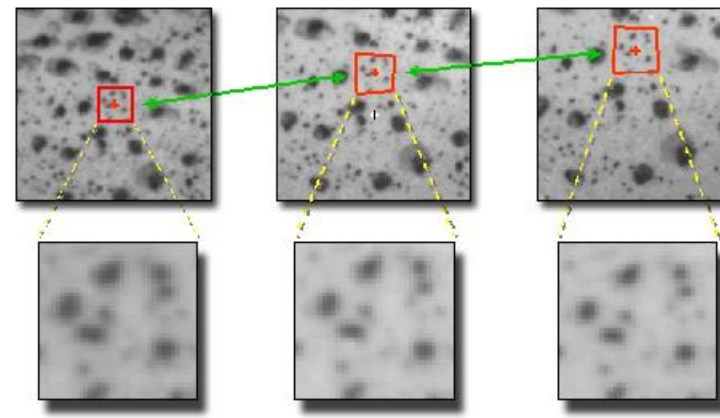

Undeformed

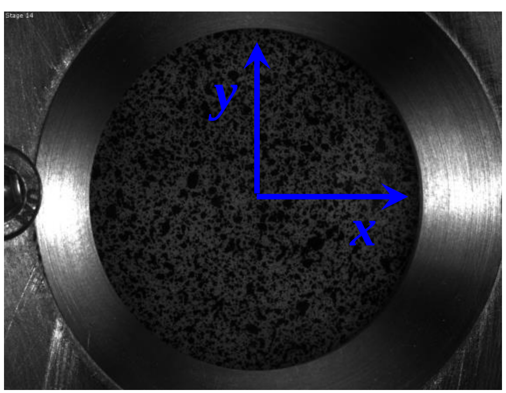

Deformed

Rupture profiles

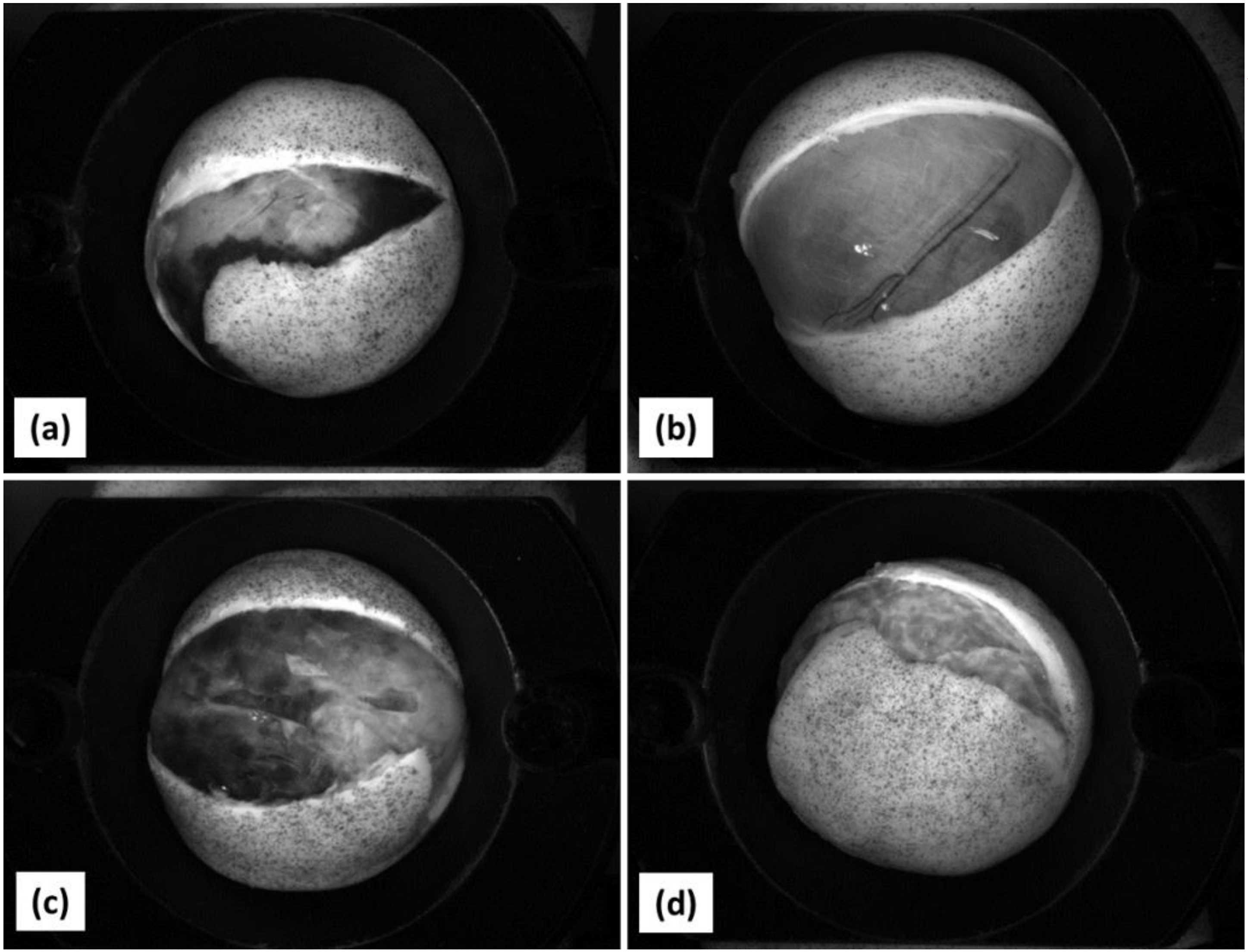

Blood flow

50% of aortas ruptured with an angle θ equal to 90 °

avril@emse.fr

Identification of local material properties

THE UNIVERSITY OF IOWA

The WHITAKER Foundation

Davis et al. BMMB – 2015.
Davis et al. JMBBM – 2016
Zhao et al. Acta Biomaterialia - 2016

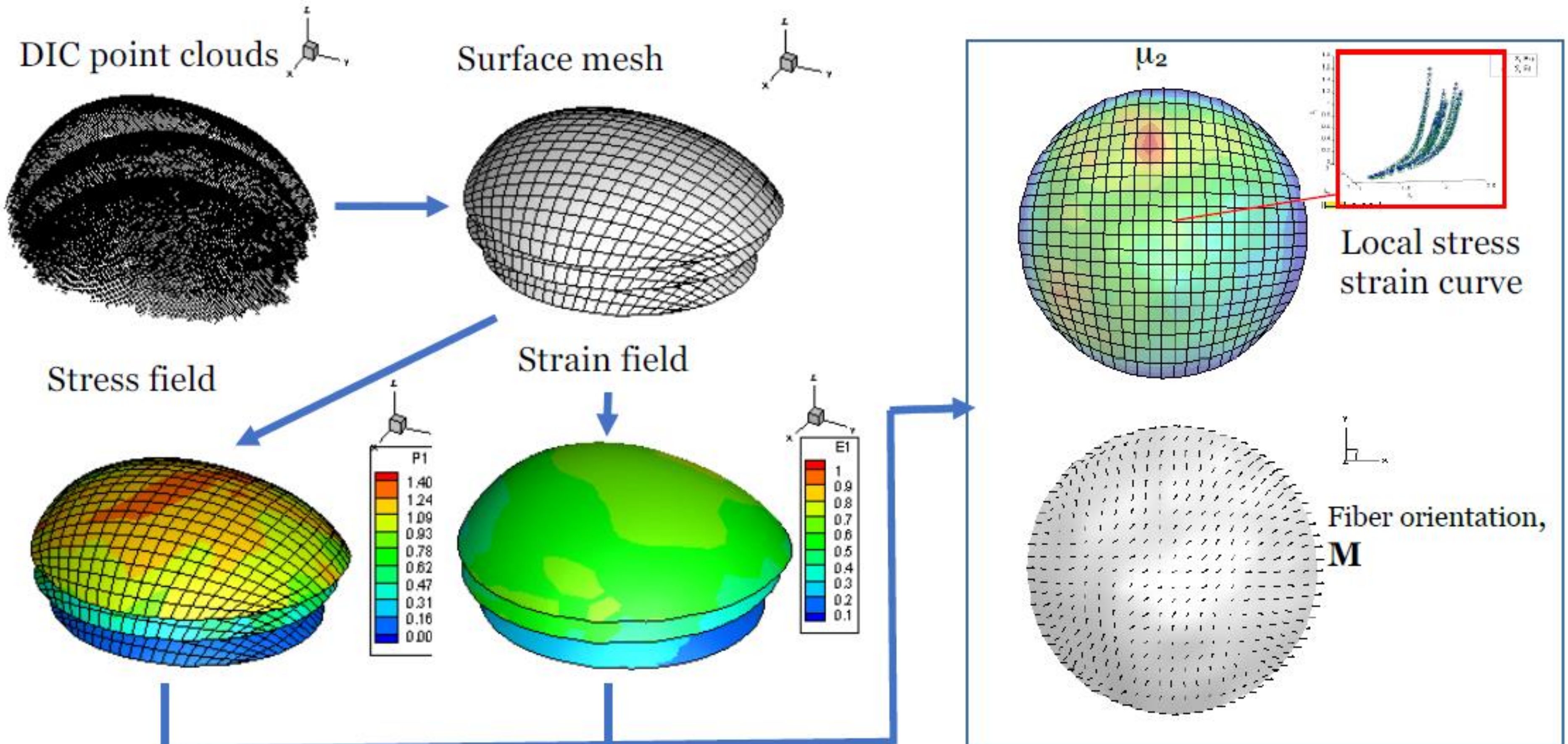

Rupture risk estimation

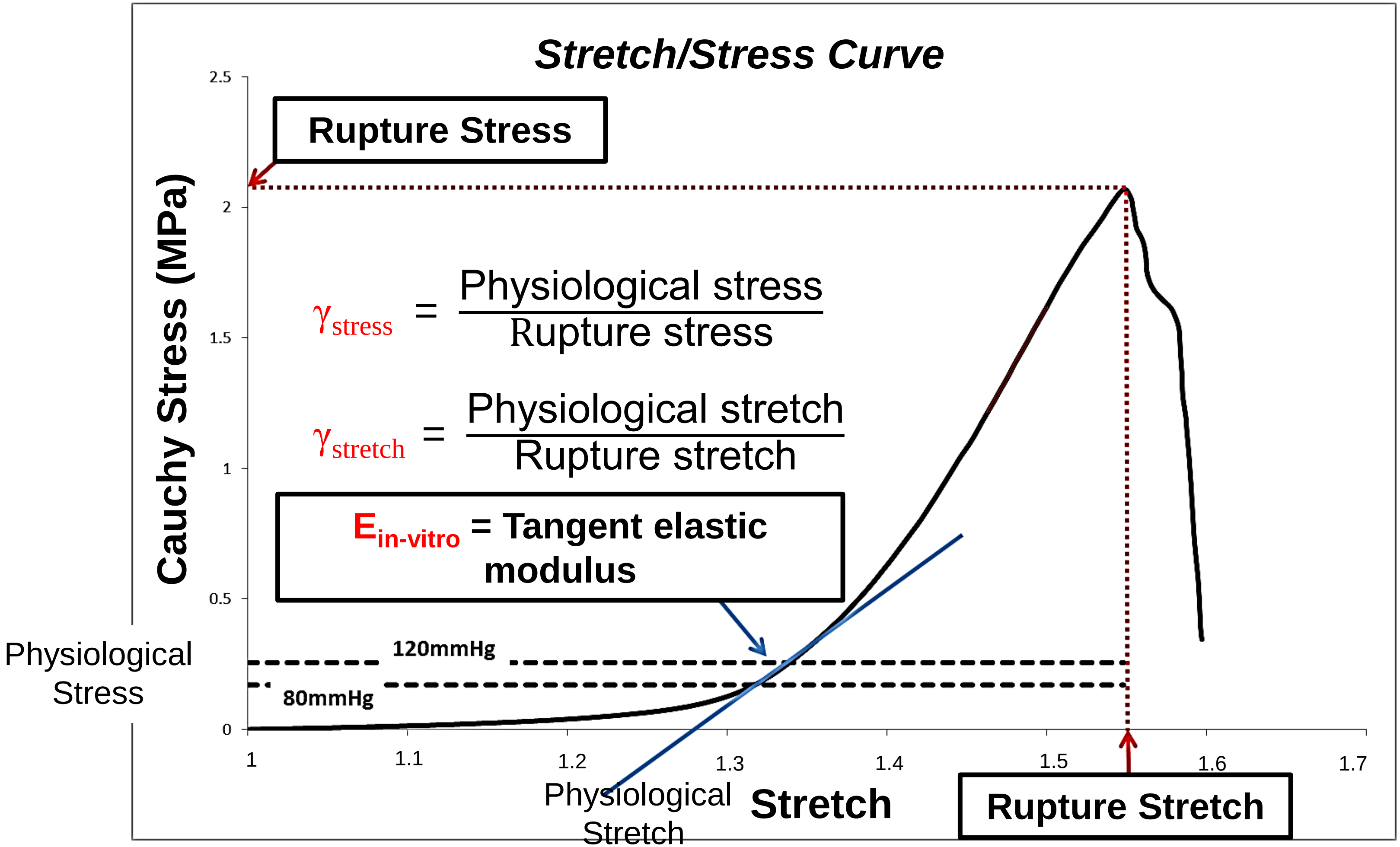

MINES Saint-Étienne

Correlation between the stretch-based rupture risk and the tangent elastic modulus

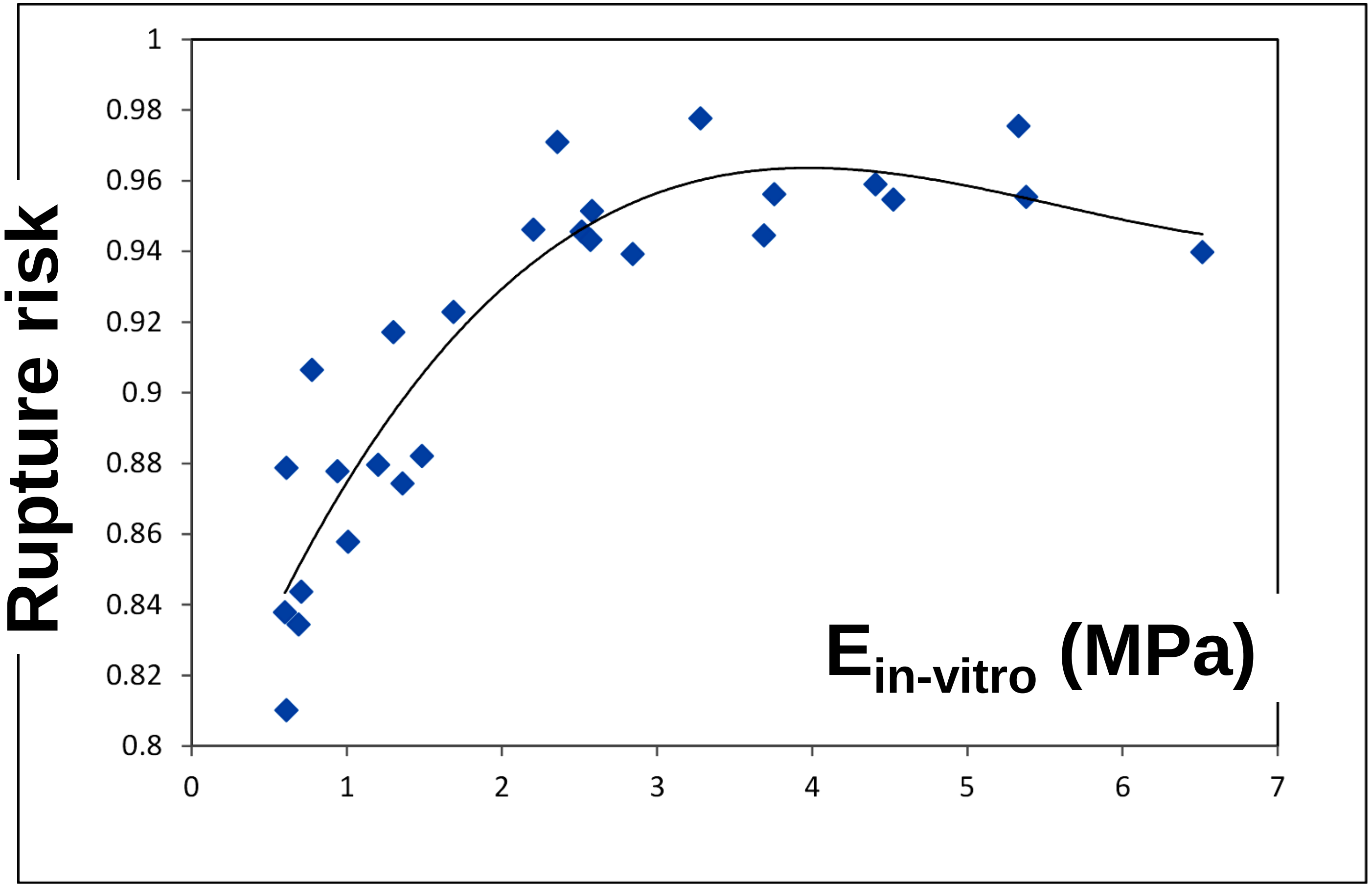

Duprey A, et al. Biaxial rupture properties of ascending thoracic aortic aneurysms. ***Acta Biomaterialia 2016.***

Relationship with hemodynamics

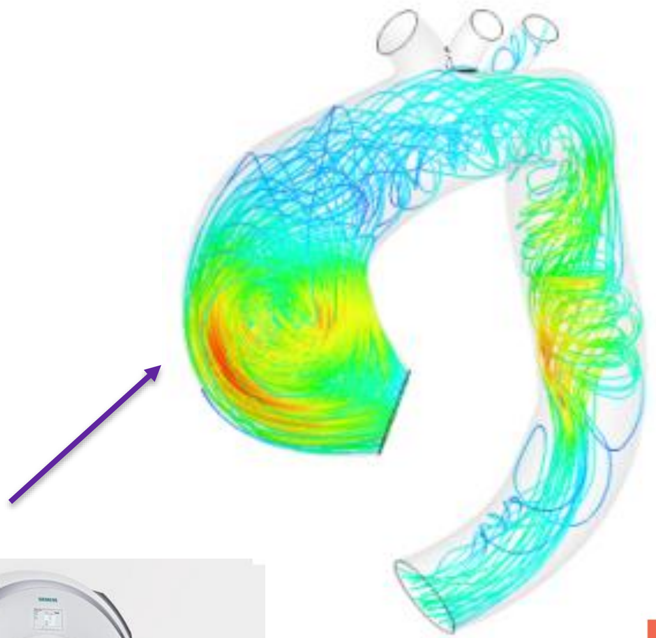

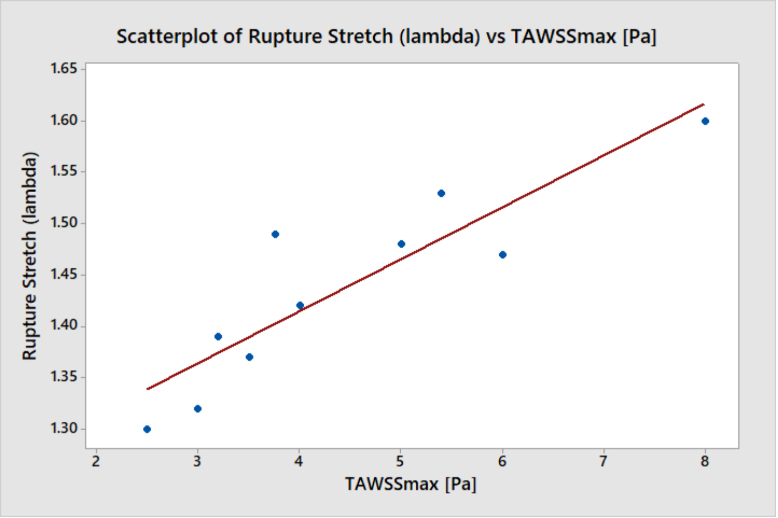

Siemens 3T Prisma

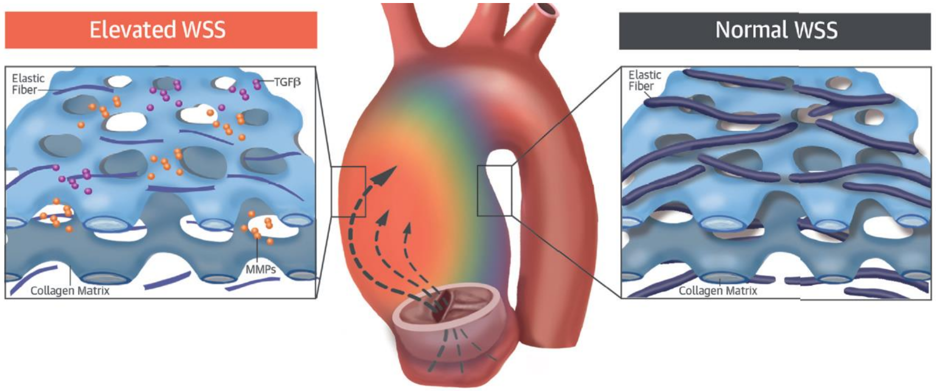

Guzzardi, D.G. et al. J Am Coll Cardiol. 2015; 66(8):892-900.

Understanding aneurysm growth using experimental mechanobiology

avril@emse.fr

What developmental biology tells us?

"Here and elsewhere we shall not obtain the best insights into things until we actually see them growing from the beginning"
Aristotle (384-322 B.C.)

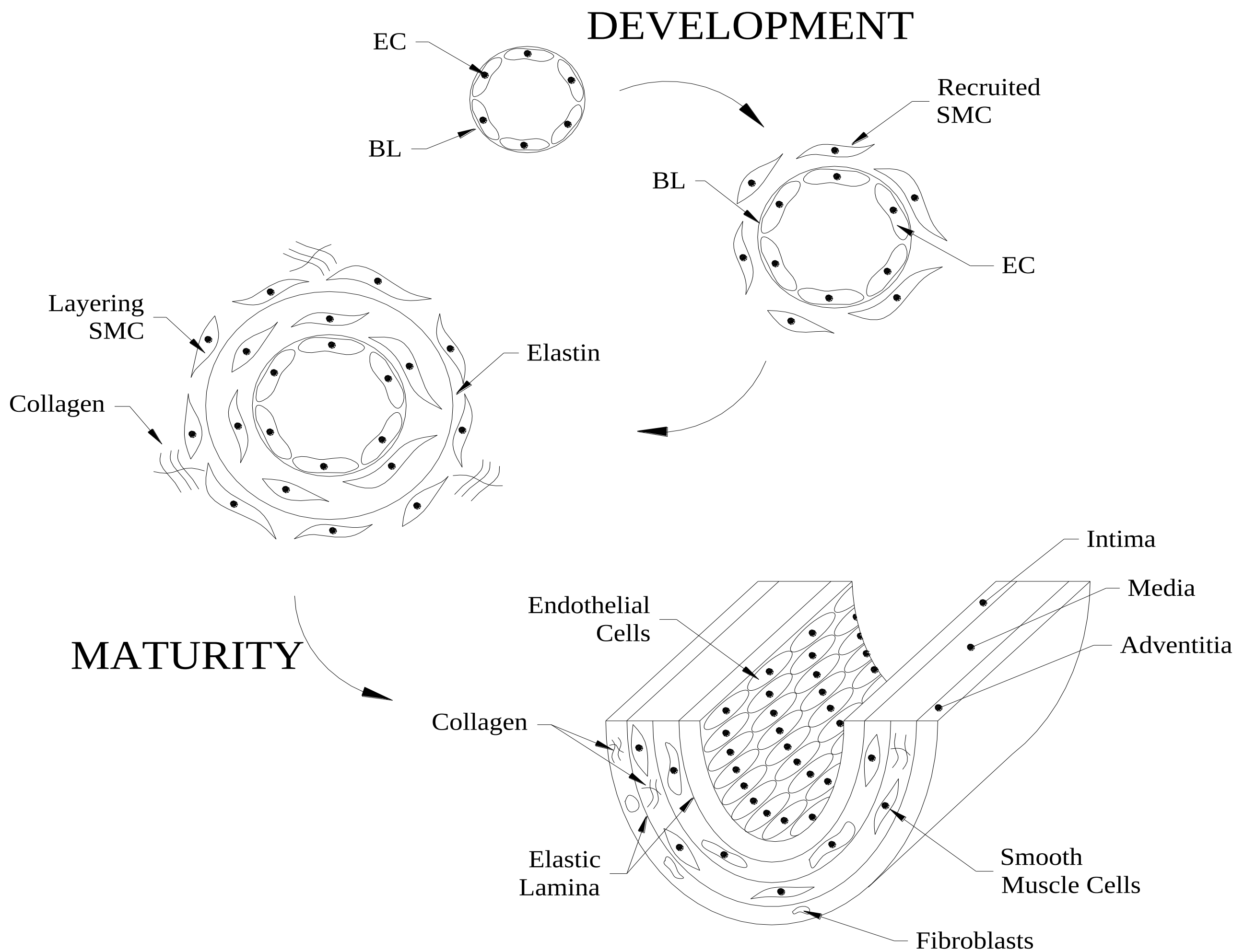

APPROACH

1. Experiments
2. Material model
3. Inverse method

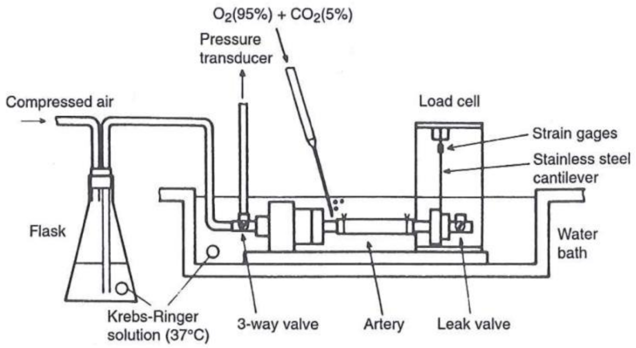

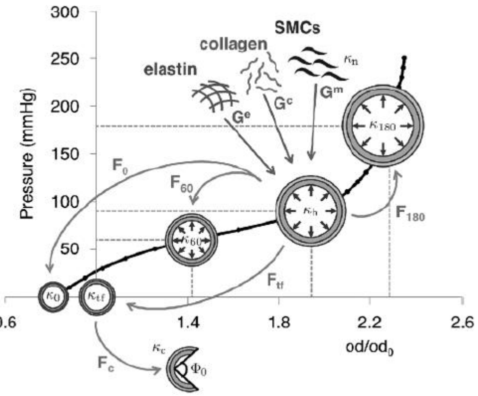

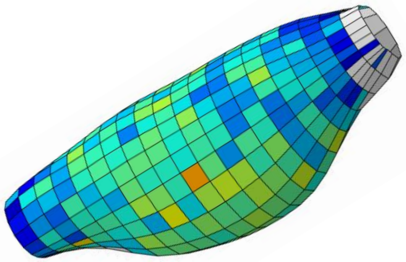

avril@emse.fr

MINES Saint-Étienne

Functional biomechanical behavior

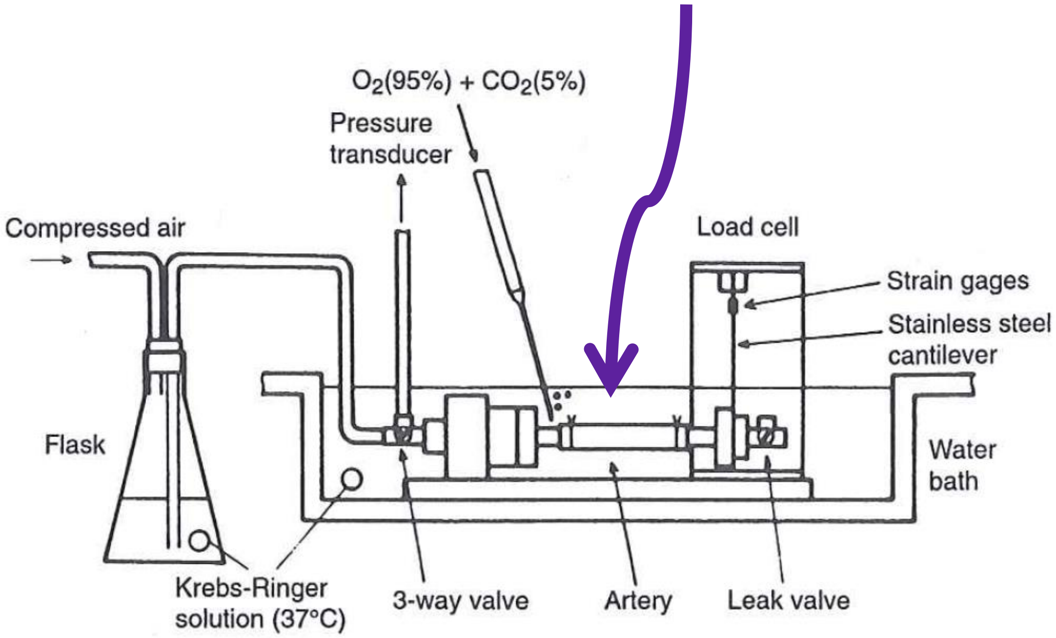

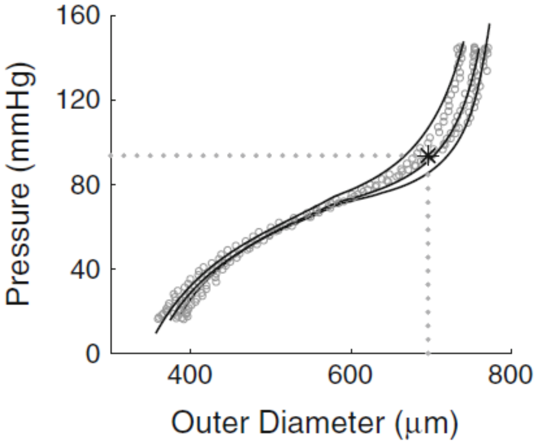

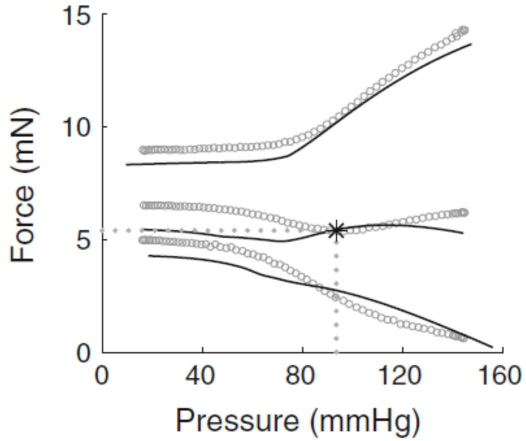

avril@emse.fr

MINES Saint-Étienne

Study Design

Control

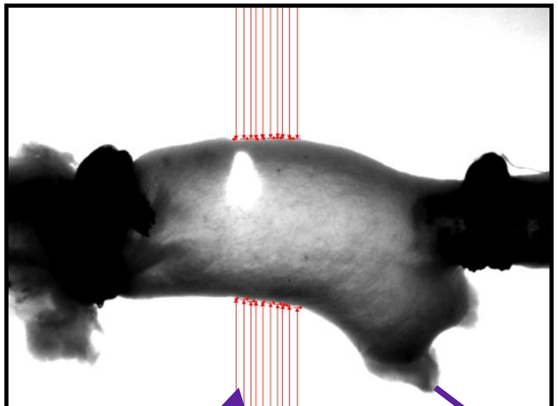

Fibulin 4 SMC KO

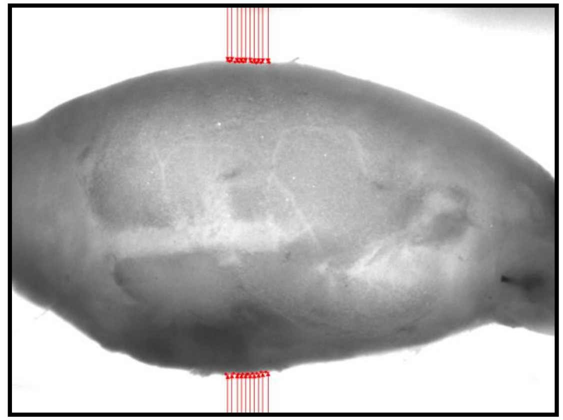

Fibrillin 1 *mgR/mgR*

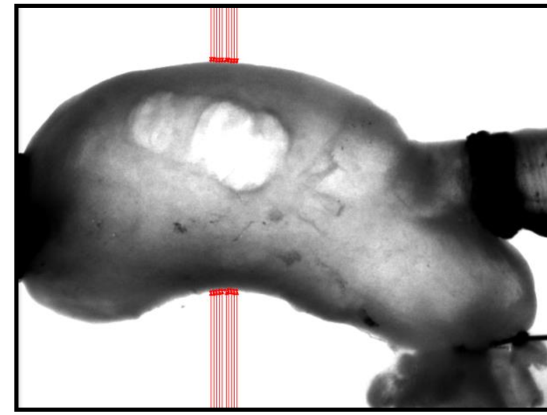

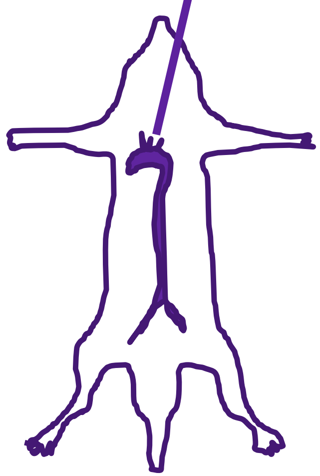

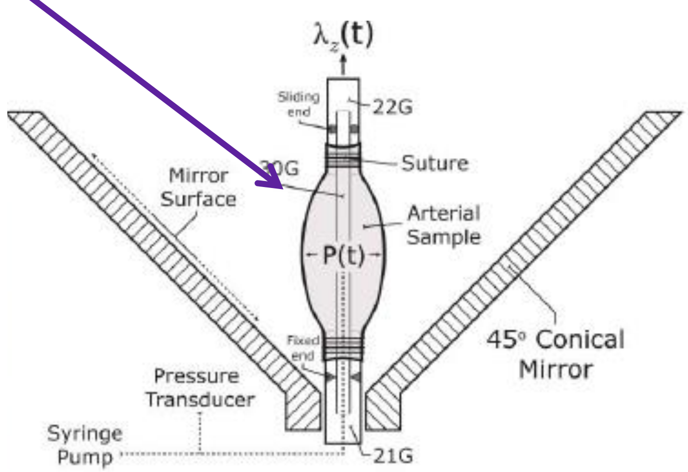

MEASUREMENT OF THE RESPONSE USING DIGITAL IMAGE CORRELATION

classical

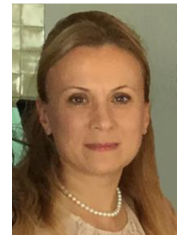

panoramic

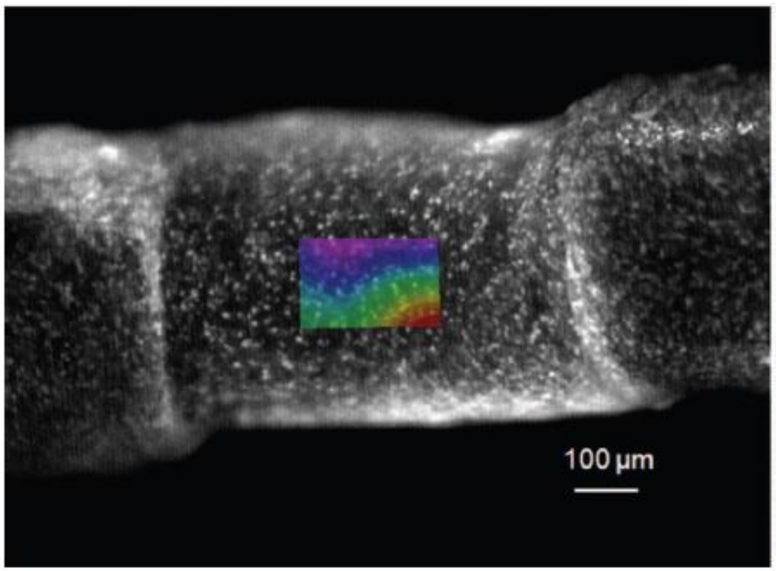

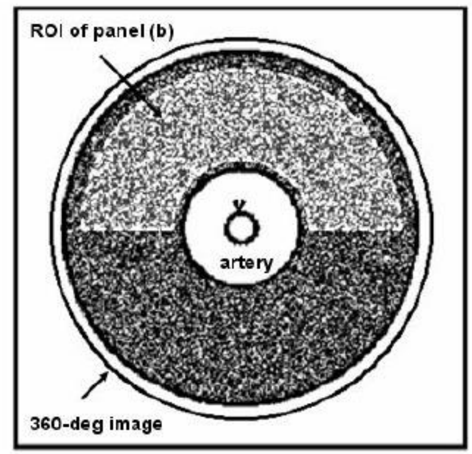

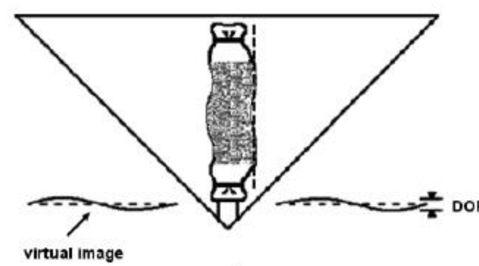

Badel et al. CMBBE, **15**, p 37-48, 2012.

Genovese. Optics Lasers Eng, **47**, p 995-1008, 2009.

The pDIC technique

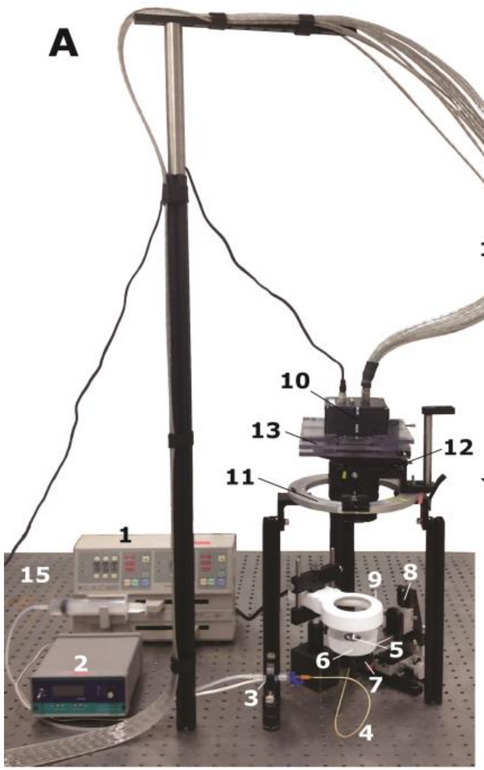

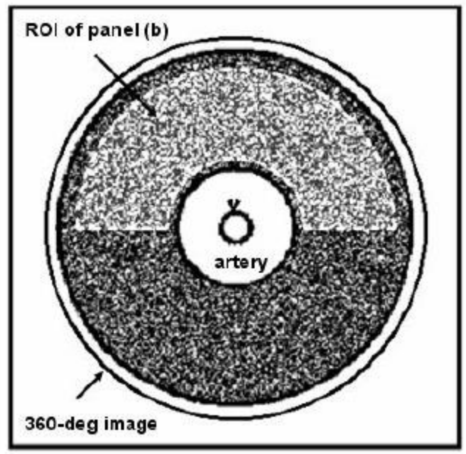

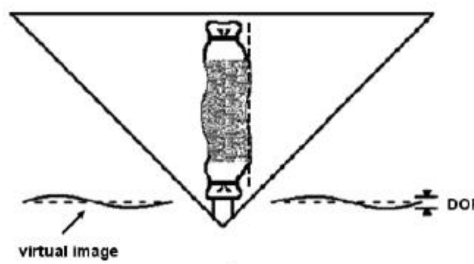

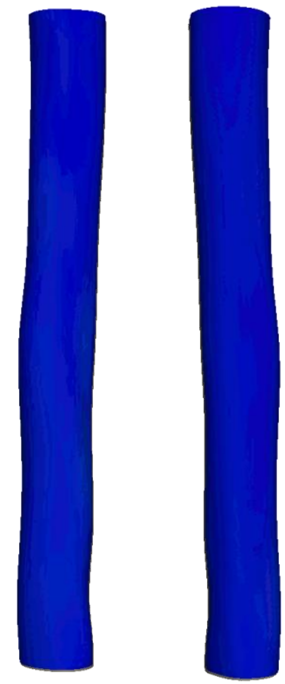

Posterior Anterior

avril@emse.fr

MINES Saint-Étienne

pDIC measurements

Fibulin 4 SMC KO

ventral *dorsal* *inflation*

6852

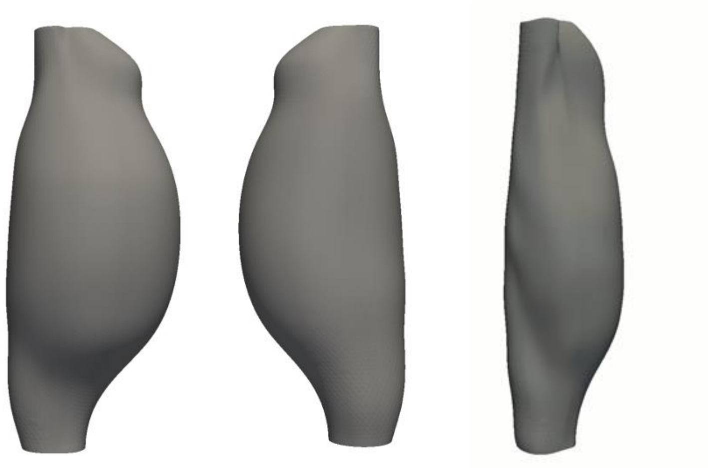

Fibrillin 1 *mgR/mgR*

ventral *dorsal* *inflation*

CS38

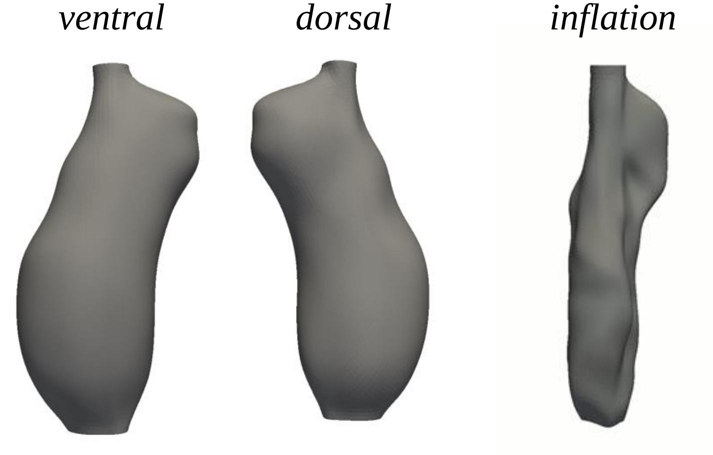

avril@emse.fr

OCT-DVC applied to arterial mechanics

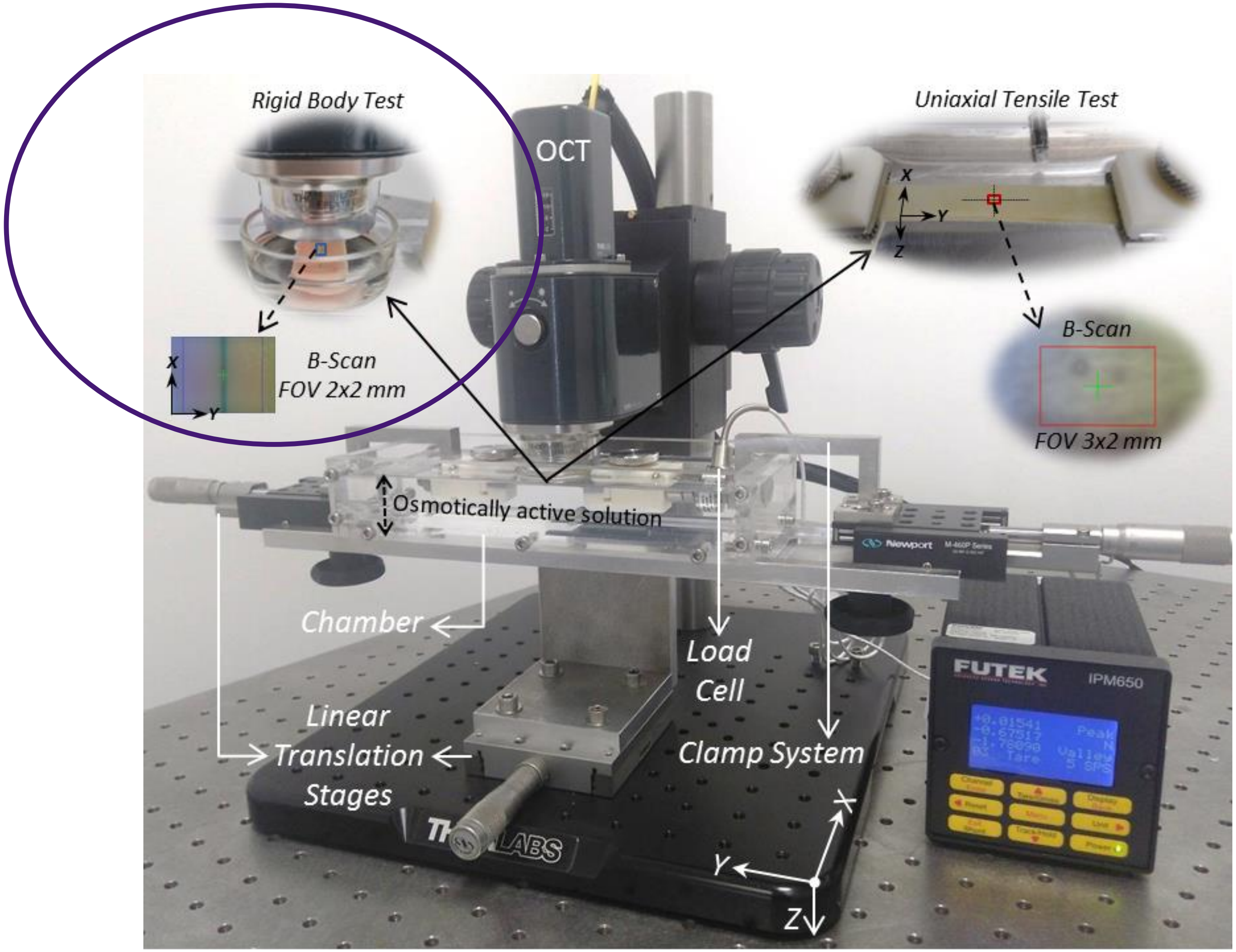

MINES Saint-Étienne

Measurement of bulk deformation fields by Digital Volume Correlation on OCT images

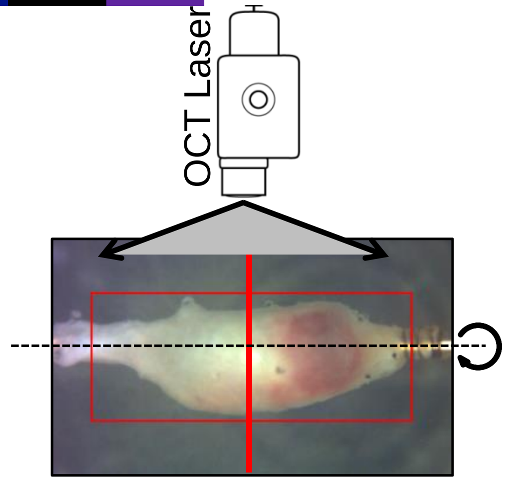

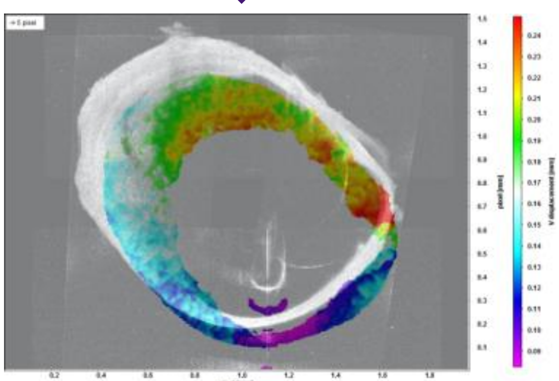

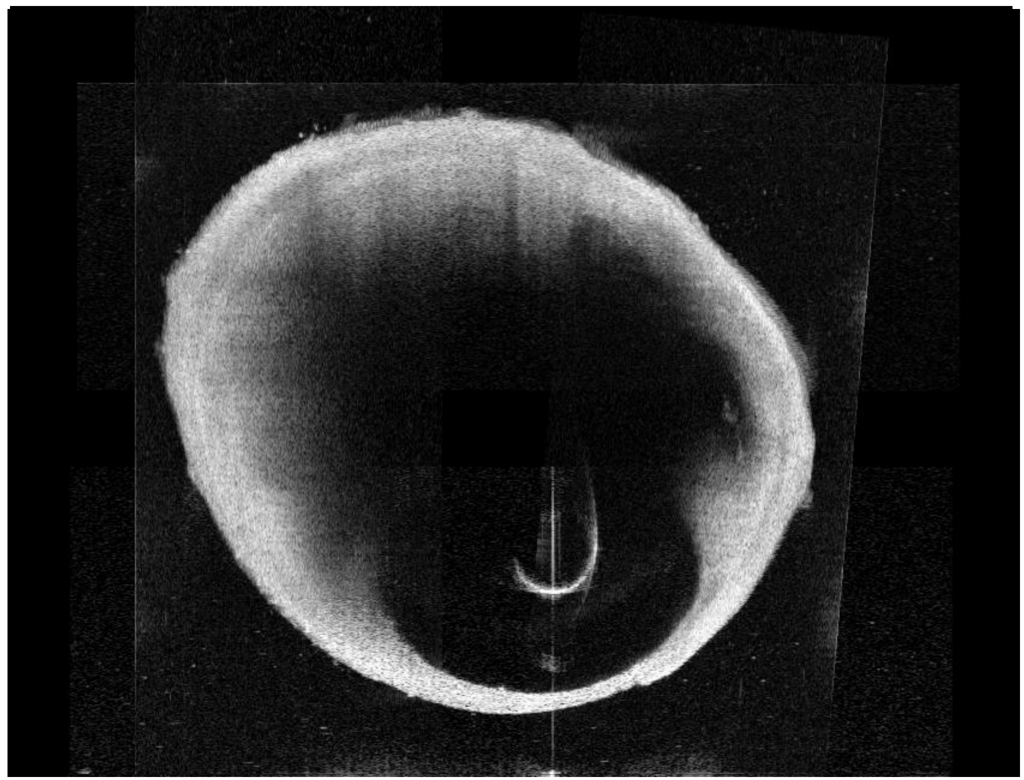

avril@emse.fr

Image Processing Methodology – Inflation Test

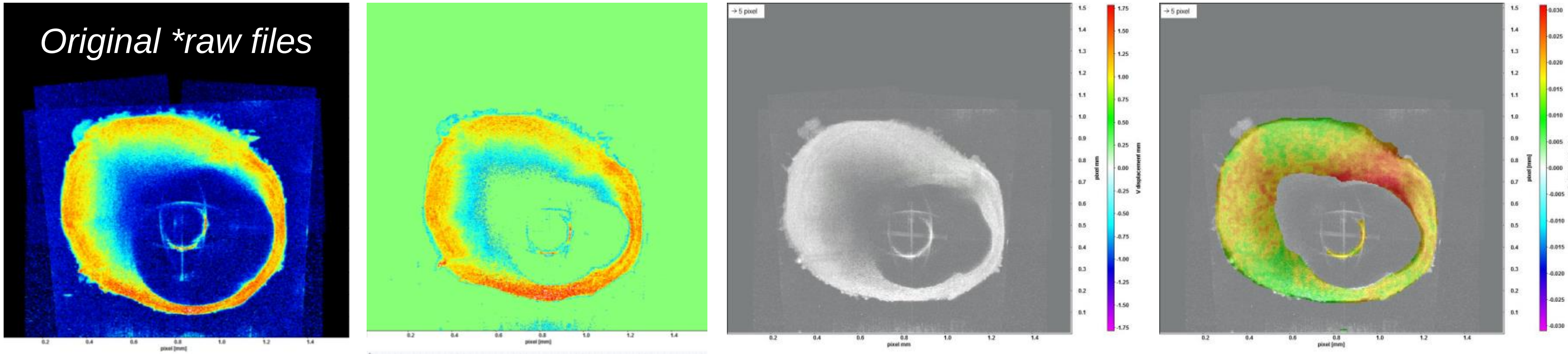

Title: REF
Width: 667 pixels
Height: 640 pixels
Depth: 100 pixels
Voxel size: 1x1x1 pixel^3 (2.38um)

Original Image Parameters

Pressures: 20, 40, 60, 80, 100, 120, 140
Lambda (λ) 1 – 2 – 3

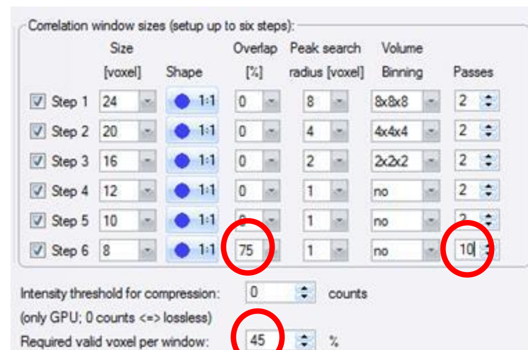

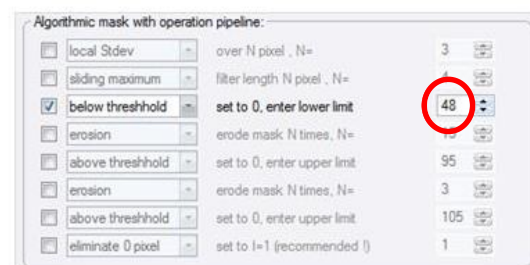

- ***Algorithmic Mask – Threshhold: 48***
- ***Correlation window size [voxel]: 24 (8x8x8)***
- ***Overlap : 75%***
- ***Passes : 10***
- ***Required valid voxel per window: 44%***

avril@emse.fr

MINES Saint-Étienne

APPROACH

1. Experiments
2. Material model
3. Inverse method

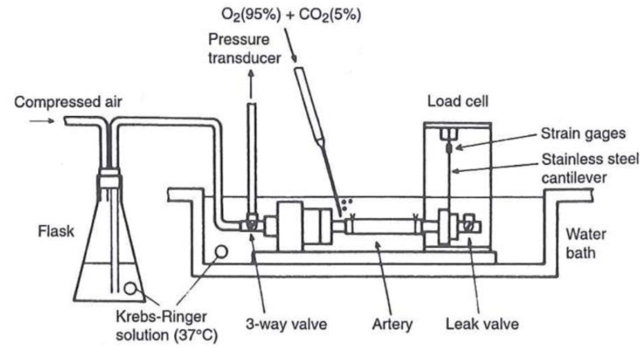

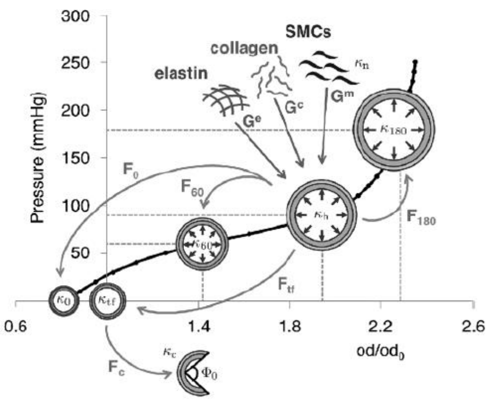

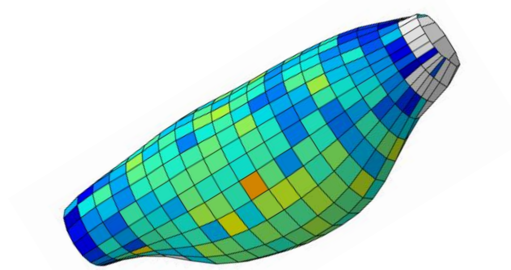

CONSTITUTIVE MODEL

Bellini, et al., Ann. Biomed. Eng., **42**(3), pp. 488–502, 2014

Strain energy functions:

$$W = \phi^{\mathrm{e}} W^{\mathrm{e}}(\mathbf{F}^{\mathrm{e}}) + \phi^{\mathrm{m}} W^{\mathrm{m}}(\lambda^{\mathrm{m}}) + \sum_{j=1}^{4} \phi^{\mathrm{c}_j} W^{\mathrm{c}_j}(\lambda^{\mathrm{c}_j})$$

$$W^{\mathrm{e}}(\mathbf{F}^{\mathrm{e}}) = \frac{c^{\mathrm{e}}}{2}\left[\mathrm{tr}\left((\mathbf{F}^{\mathrm{e}})^{\mathrm{T}}\mathbf{F}^{\mathrm{e}}\right) - 3\right]$$

$$W^{\mathrm{m}}(\lambda^{\mathrm{m}}) = \frac{c_2^{\mathrm{m}}}{4c_3^{\mathrm{m}}}\left[e^{c_3^{\mathrm{m}}\left((\lambda^{\mathrm{m}})^2-1\right)^2} - 1\right]$$

$$W^{\mathrm{c}}(\lambda^{\mathrm{c}_j}) = \frac{c_2^{\mathrm{c}}}{4c_3^{\mathrm{c}}}\left[e^{c_3^{\mathrm{c}}\left((\lambda^{\mathrm{c}_j})^2-1\right)^2} - 1\right]$$

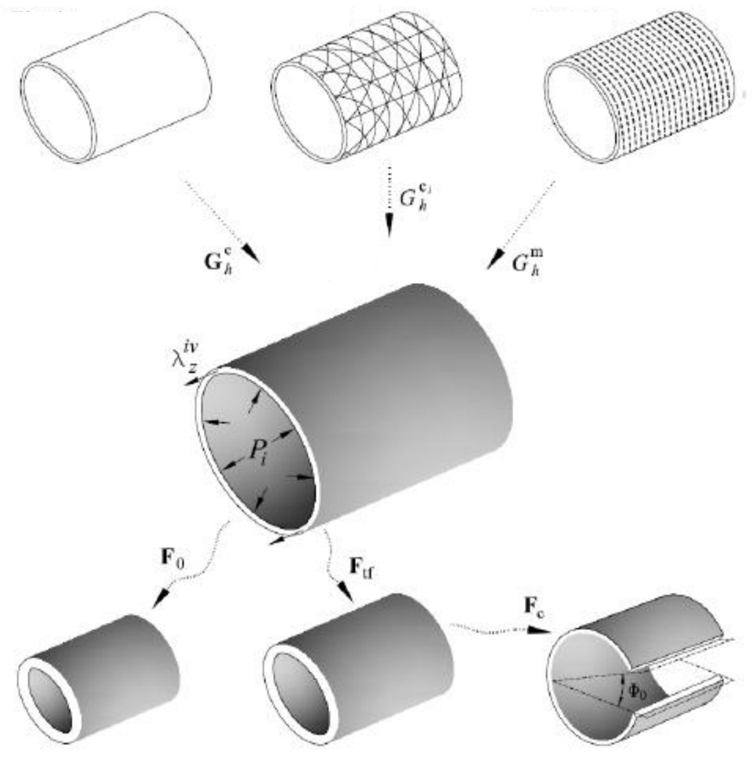

avril@emse.fr

MINES Saint-Étienne

PARAMETERS TO BE IDENTIFIED

$$W = \phi^{e} W^{e}(\mathbf{F}^{e}) + \phi^{m} W^{m}(\lambda^{m}) + \sum_{j=1}^{4} \phi^{c_j} W^{c_j}(\lambda^{c_j})$$

$$W^{e}(\mathbf{F}^{e}) = \frac{c^{e}}{2}\left[\mathrm{tr}\left((\mathbf{F}^{e})^{T}\mathbf{F}^{e}\right) - 3\right]$$

$$W^{m}(\lambda^{m}) = \frac{c_2^{m}}{4c_3^{m}}\left[e^{c_3^{m}((\lambda^{m})^2-1)^2} - 1\right]$$

$$W^{c}(\lambda^{c_j}) = \frac{c_2^{c}}{4c_3^{c}}\left[e^{c_3^{c}((\lambda^{c_j})^2-1)^2} - 1\right]$$

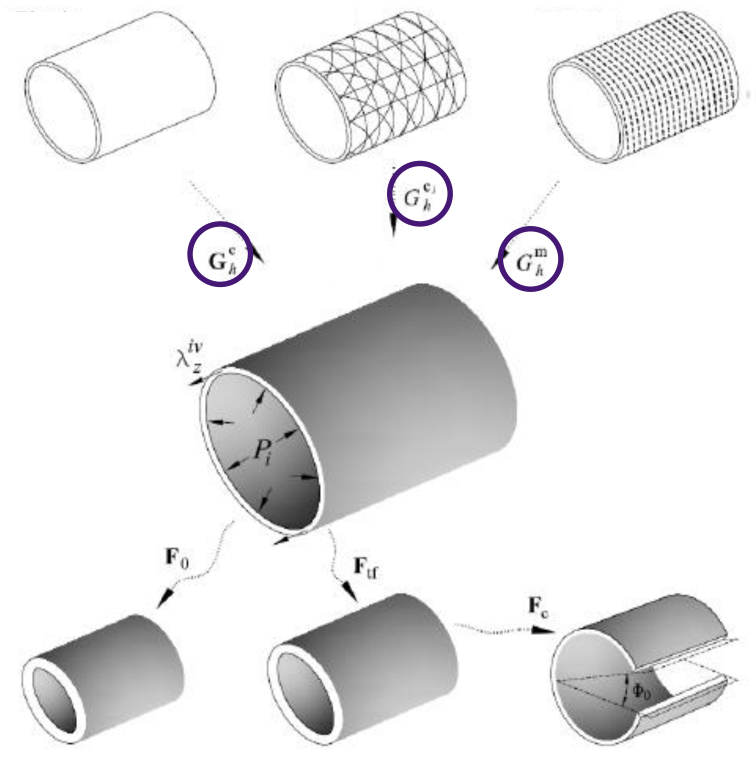

avril@emse.fr

MINES Saint-Étienne

APPROACH

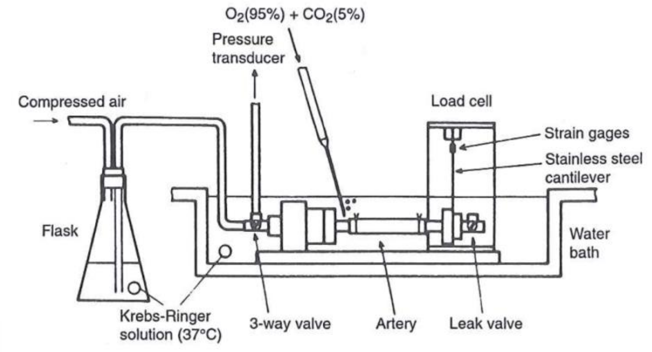

1. Experiments
2. Material model
3. Inverse method

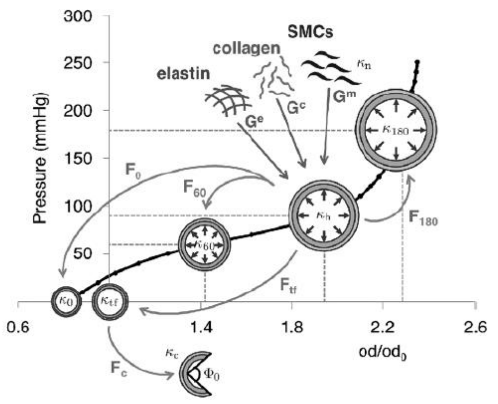

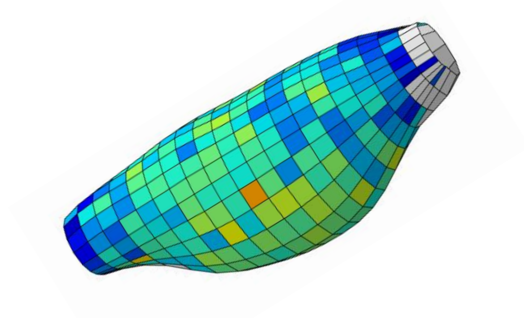

avril@emse.fr

MINES Saint-Étienne

Inverse approach – traditional approach

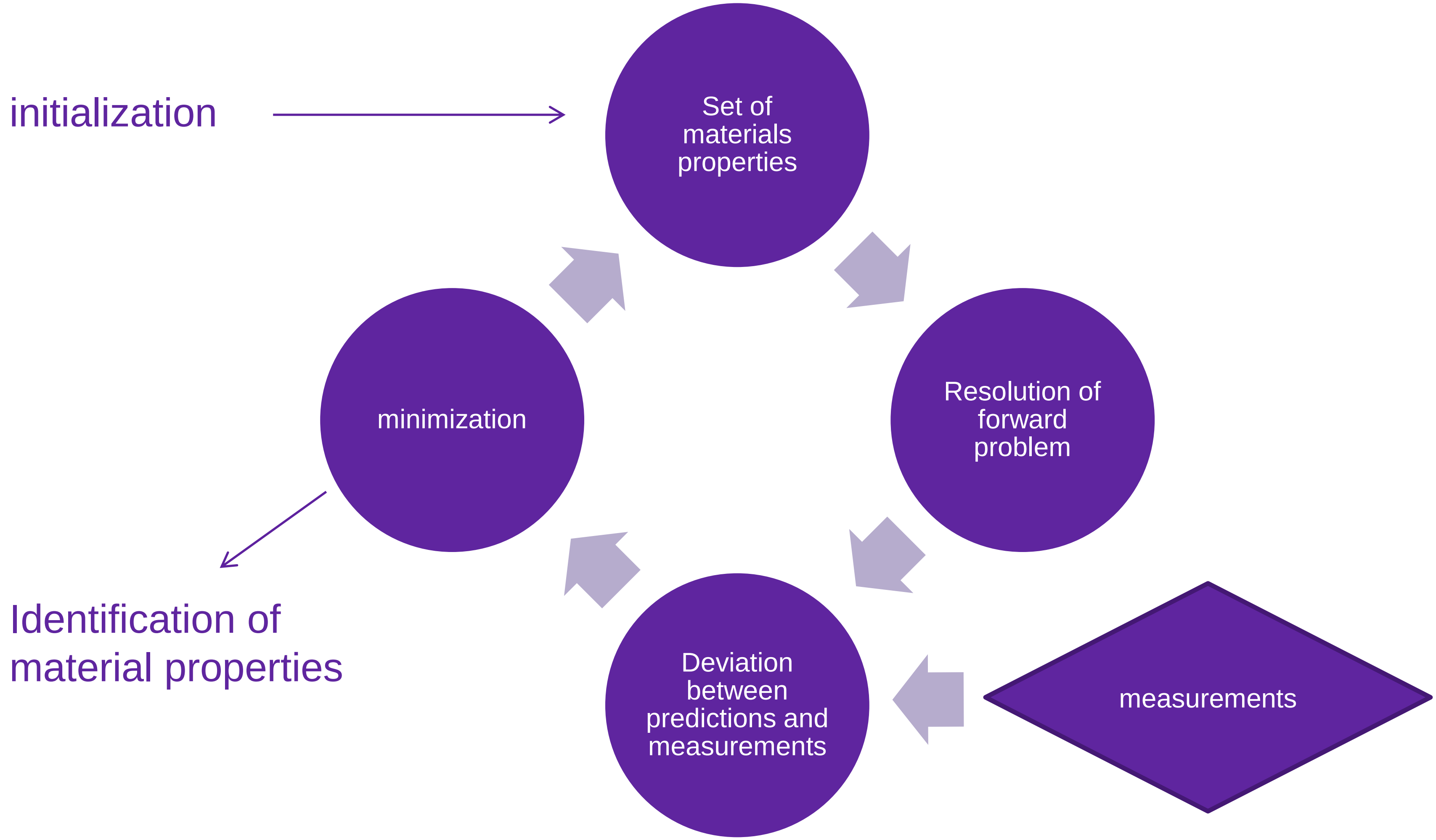

avril@emse.fr

Inverse approach – FEMU approach

initialization →

Set of materials properties

Oberai et al., Inverse problems, **19**, pp. 297-313, 2003

Resolution of forward problem

Deviation between predictions and measurements

measurements

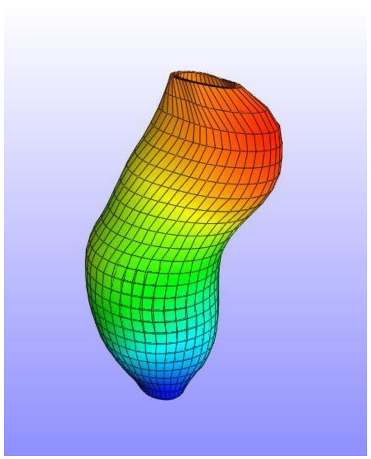

$$J(\mu) = \|T(u) - T(u^{exp})\|^2 + \frac{\alpha}{2} B(\mu)$$

avril@emse.fr

Inverse approach – FEMU approach

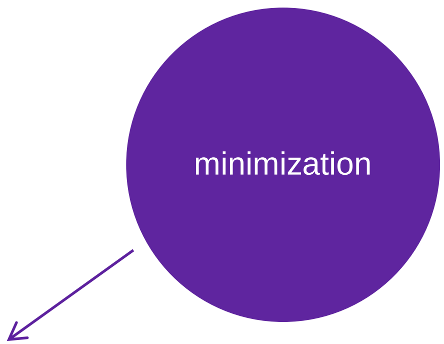

Identification of material properties

1. Use a gradient based method (steepest descent or BFGS)

2. Need to derive the gradient of J with respect to μ at each iteration. With the adjoint method, this requires the resolution of 2 forward problems

3. Very unstable with hyperelastic models: **many risks that the forward problems have a poor convergence**

avril@emse.fr

MINES Saint-Étienne

Alternative inverse approach: the virtual fields method

initialization

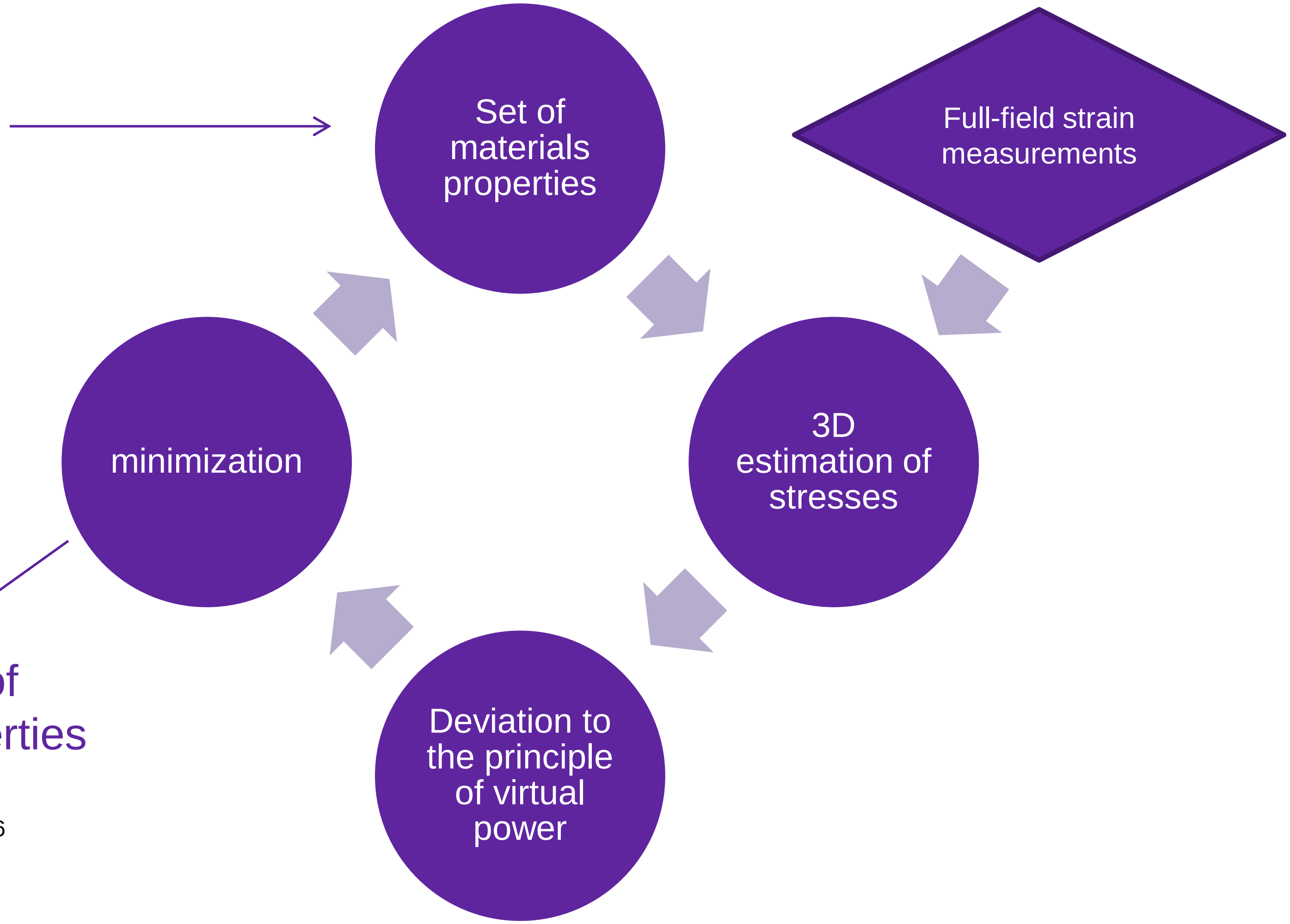

Identification of material properties

Bersi et al., J Biomech Eng, 2016

Full-field stress reconstruction

initialization

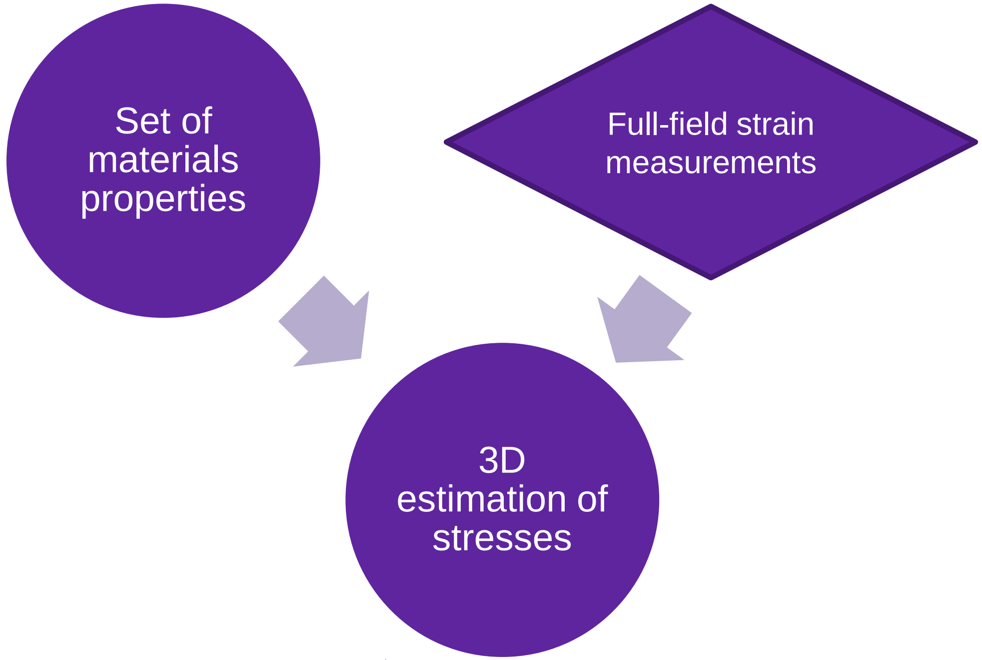

$$W = \phi^{e} W^{e}(\mathbf{F}^{e}) + \phi^{m} W^{m}(\lambda^{m}) + \sum_{j=1}^{4} \phi^{c_j} W^{c_j}(\lambda^{c_j})$$

$$W^{e}(\mathbf{F}^{e}) = \frac{c^{e}}{2}\left[\mathrm{tr}\left((\mathbf{F}^{e})^{T}\mathbf{F}^{e}\right) - 3\right]$$

$$W^{m}(\lambda^{m}) = \frac{c_2^{m}}{4c_3^{m}}\left[e^{c_3^{m}\left((\lambda^{m})^2-1\right)^2} - 1\right]$$

$$W^{c}(\lambda^{c_j}) = \frac{c_2^{c}}{4c_3^{c}}\left[e^{c_3^{c}\left((\lambda^{c_j})^2-1\right)^2} - 1\right]$$

Simple application of the constitutive model for each element

avril@emse.fr

Minimization of the equilibrium gap using the principle of virtual power

minimization

$$J = \sum_{p} \sum_{\lambda} \Bigg(\underbrace{- \int_{\omega(t)} \underline{\underline{\sigma}} : \left(\underline{\nabla} \otimes \underline{\xi}^{*} \right) d\omega}_{P^{*}_{int}} + \underbrace{\oint_{\partial\omega(t)} \underline{T} : \underline{\xi}^{*} \, ds}_{P^{*}_{ext}} \Bigg)^{2}$$

Bersi et al., J Biomech Eng, 2016

Resolution:

$$\underbrace{\min_{c_3^1, c_3^{2,3}, c_3^4, \alpha, \beta} \Bigg[\underbrace{\min_{c^e, c_2^1, c_2^{2,3}, c_2^4} \left[\frac{J(u)}{A} + \frac{J(v)}{B} \right]}_{\text{Linear least-squares}} \Bigg]}_{\text{Genetic algorithm}}$$

avril@emse.fr

MINES Saint-Étienne

Derivation of stress tensor using layer specific constitutive behavior

3D estimation of strains

↓

3D estimation of stress

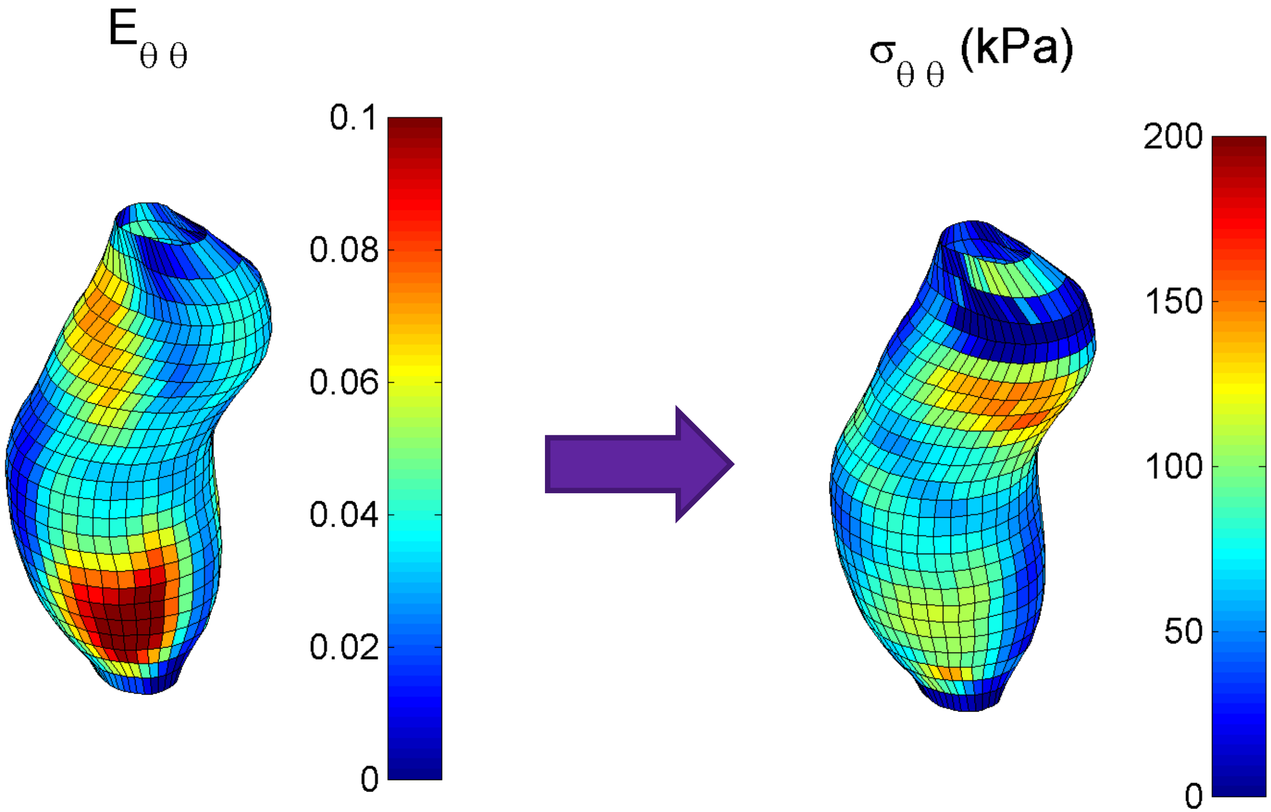

avril@emse.fr

Virtual power 1

1. A local virtual radial "bulge": $\mathbf{u}(\mathbf{x}) = [f(\mathbf{x}-\mathbf{x}_0)/r^2]\,\mathbf{e}_r$

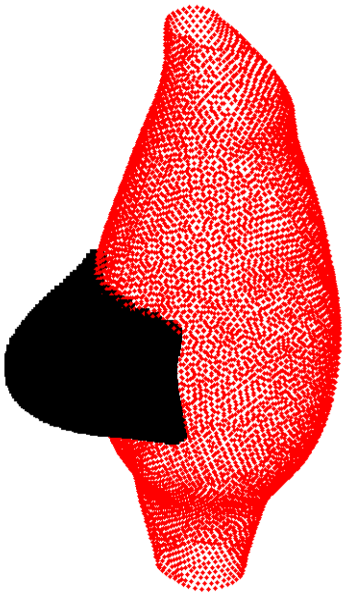

$$\underbrace{-\int_{\omega(t)} \underline{\underline{\sigma}} : \left(\underline{\nabla} \otimes \underline{\xi}^*\right) d\omega}_{P^*_{int}} + \underbrace{\oint_{\partial\omega(t)} \underline{T} : \underline{\xi}^* \, ds}_{P^*_{ext}} = 0$$

After deriving virtual strains (infinitesimal) local internal virtual work is derived at every Gauss point and integrated across the volume

The virtual field is normalized such as the external virtual work equals P.

avril@emse.fr

Virtual power 2

2. Local virtual axial extension: $\mathbf{v}(\mathbf{x}) = f(\mathbf{x}-\mathbf{x}_0)\,(z\,\mathbf{e}_z - x/2\,\mathbf{e}_x - y/2\,\mathbf{e}_y)$

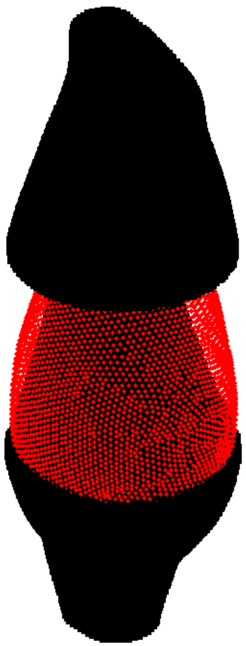

$$\underbrace{-\int_{\omega(t)} \underline{\underline{\sigma}} : \left(\underline{\nabla} \otimes \underline{\xi}^*\right) d\omega}_{P^*_{int}} + \underbrace{\oint_{\partial\omega(t)} \underline{T} : \underline{\xi}^* \, ds}_{P^*_{ext}} = 0$$

After deriving virtual strains (infinitesimal) local internal virtual work is derived at every Gauss point and integrated across the volume

The virtual field is normalized such as the external virtual work equals F.

Minimizing the equilibrium gap

minimization

$$J = \sum_{p} \sum_{\lambda} \Bigg(\underbrace{- \int_{\omega(t)} \underline{\underline{\sigma}} : \left(\underline{\nabla} \otimes \underline{\xi}^* \right) d\omega}_{P^*_{int}} + \underbrace{\oint_{\partial\omega(t)} \underline{T} : \underline{\xi}^* \, ds}_{P^*_{ext}} \Bigg)^2$$

Bersi et al., J Biomech Eng, 2016

Resolution:

$$\min_{c_3^1, c_3^{2,3}, c_3^4, \alpha, \beta} \left[\min_{c^e, c_2^1, c_2^{2,3}, c_2^4} \left[\frac{J(u)}{A} + \frac{J(v)}{B} \right] \right]$$

Linear least-squares

Genetic algorithm

avril@emse.fr

Similar to material fitting at every position

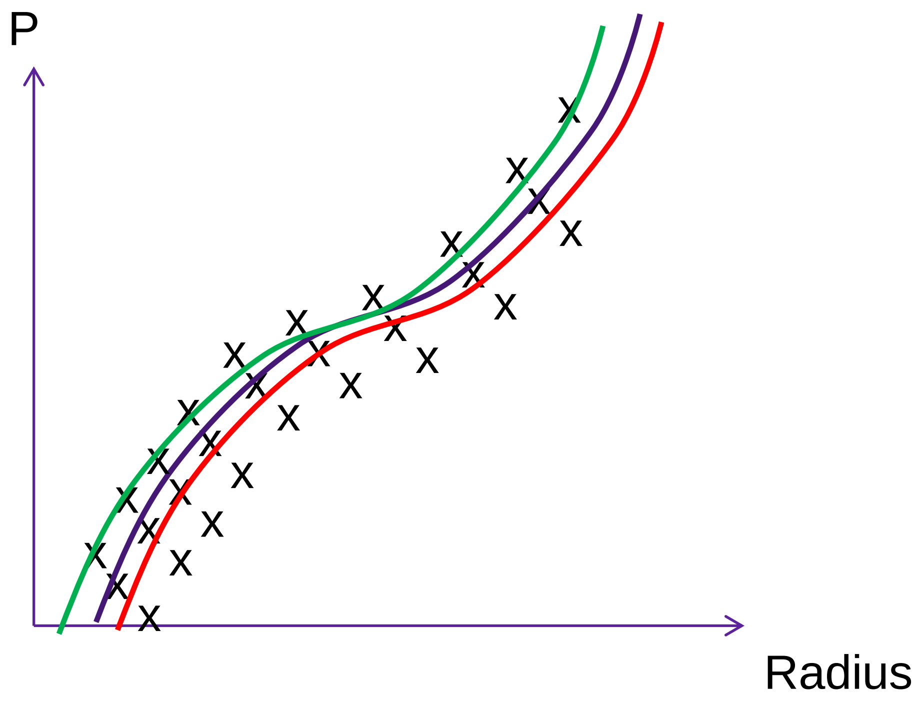

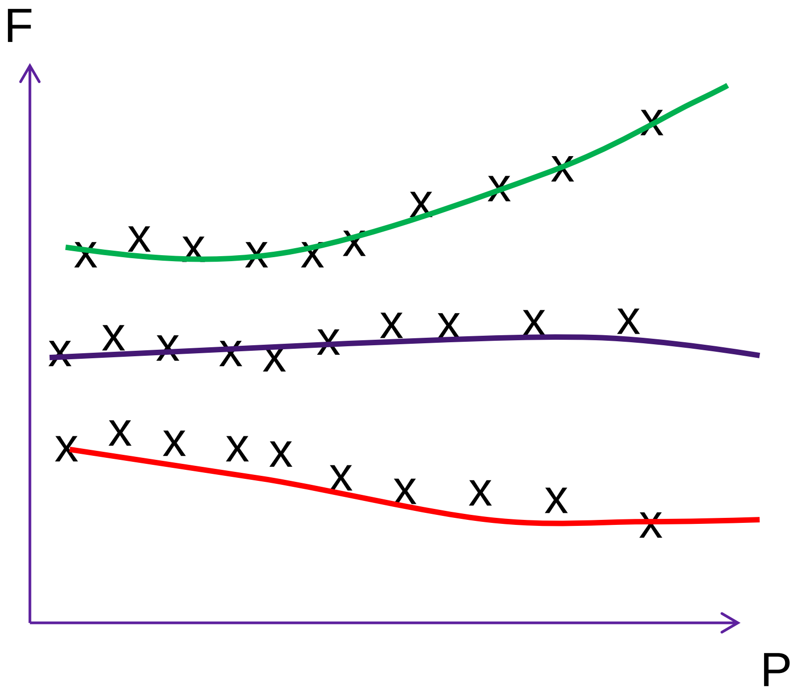

Crosses represent external virtual work for every pressure and axial stretch
Solid lines represent internal virtual work
The goodness of fit is evaluated with the R^2 value

Summary of the inverse approach

initialization

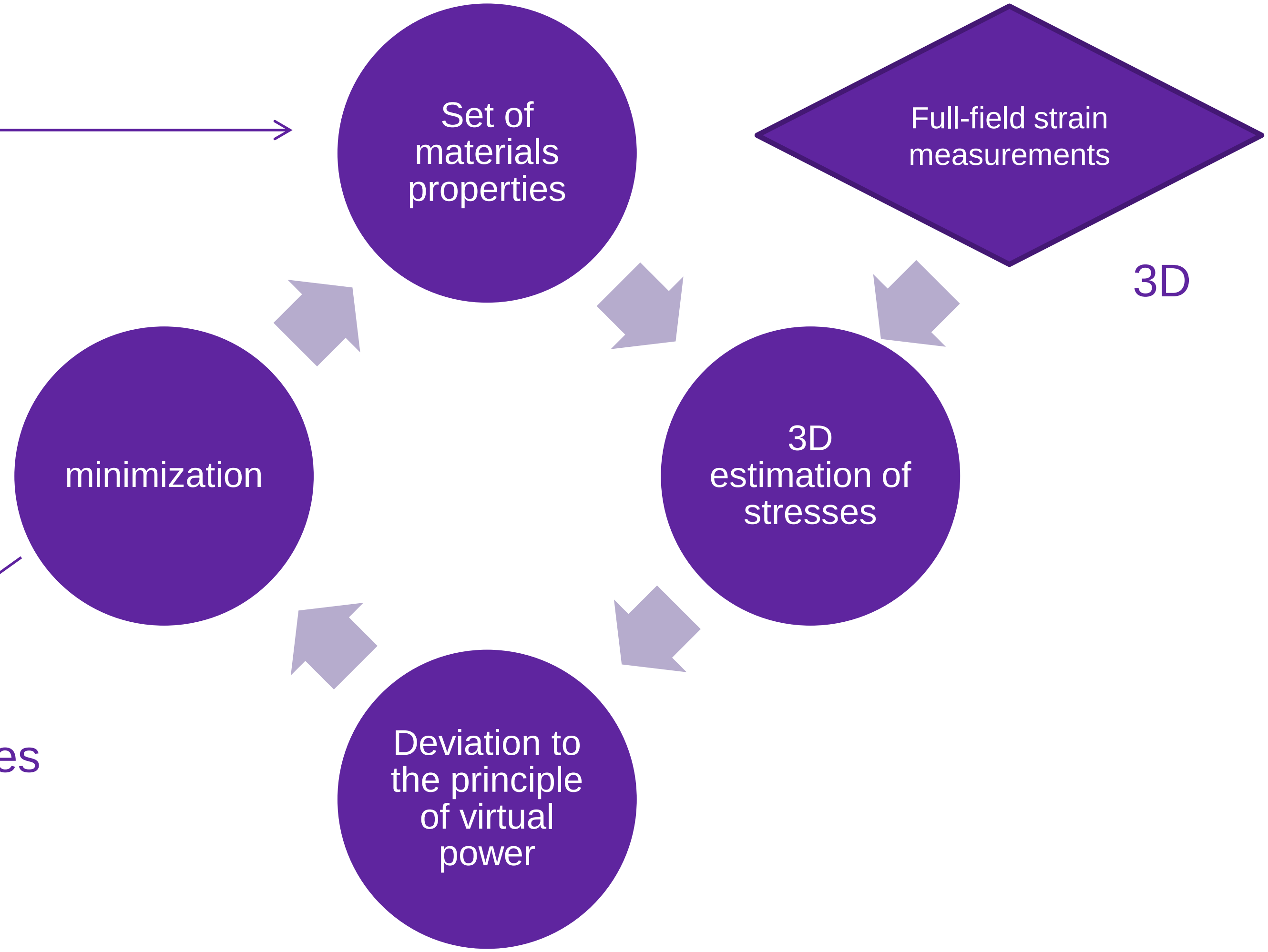

Identification of material properties

Bersi et al., J Biomech Eng, 2016
Bersi et al, BMMB, 2018

Results - Highlights

Full-Field Material Parameter Estimation vs thickness distribution

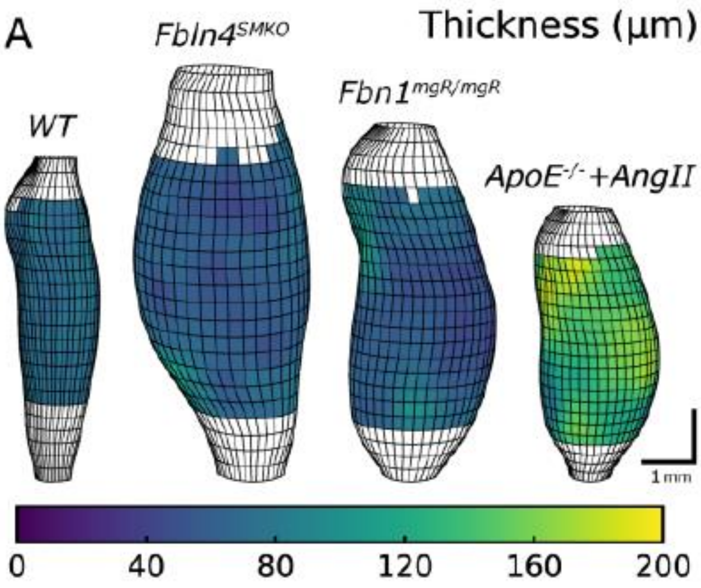

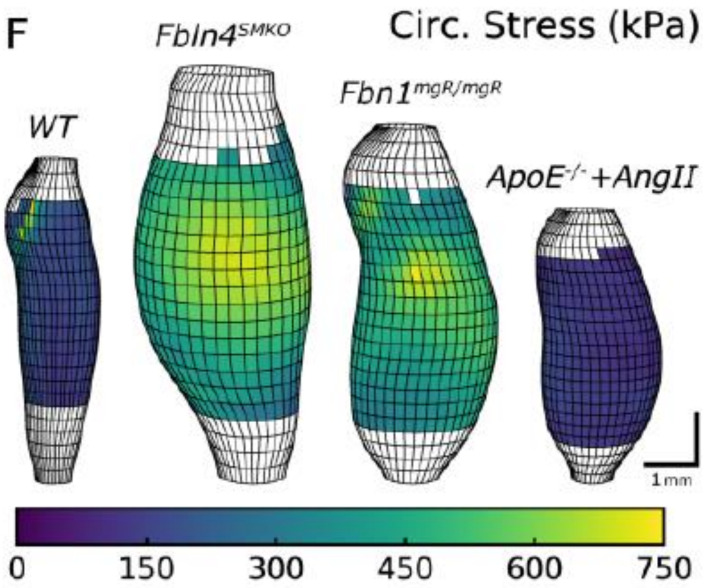

Correlation with tissue µstructure

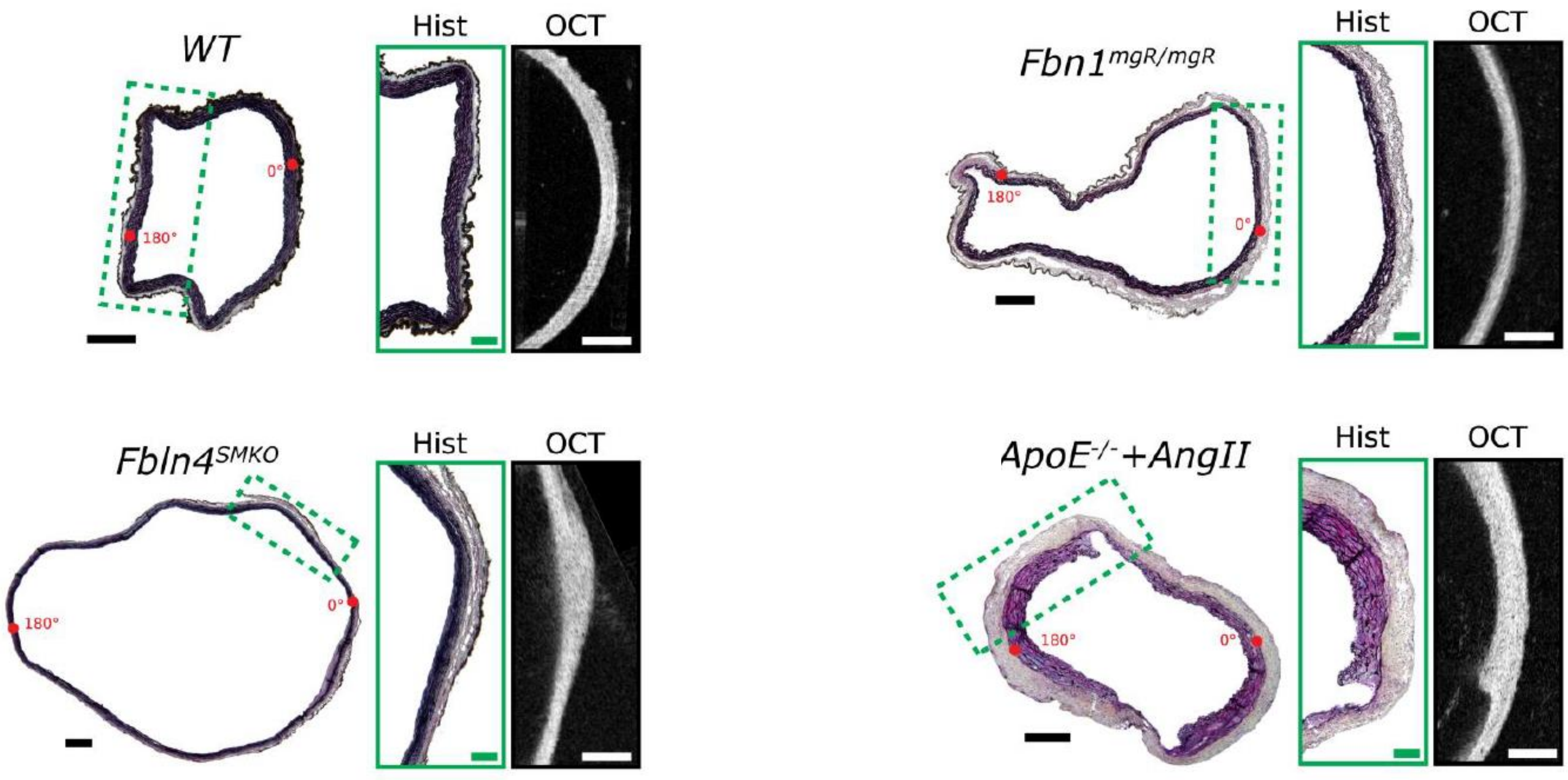

avril@emse.fr

Full-Field Material Parameter Estimation vs local stress

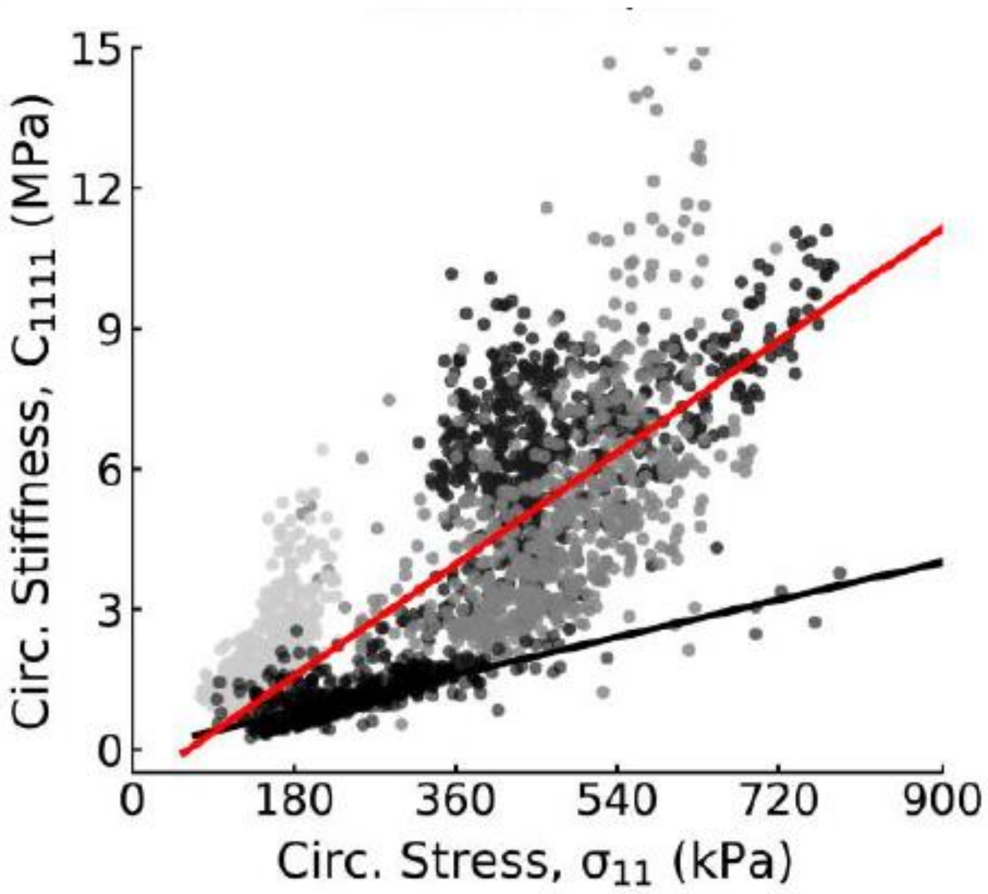

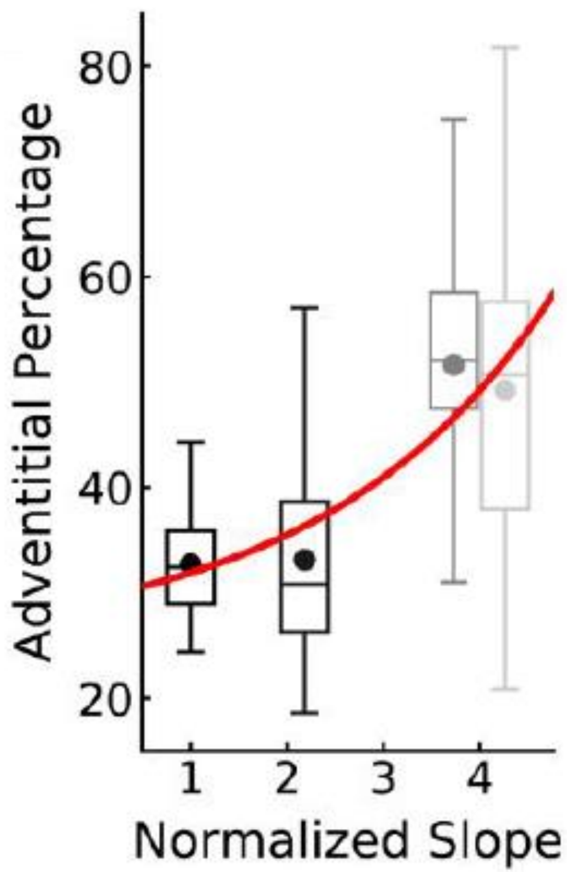

DISSECTED ANEURYSMS

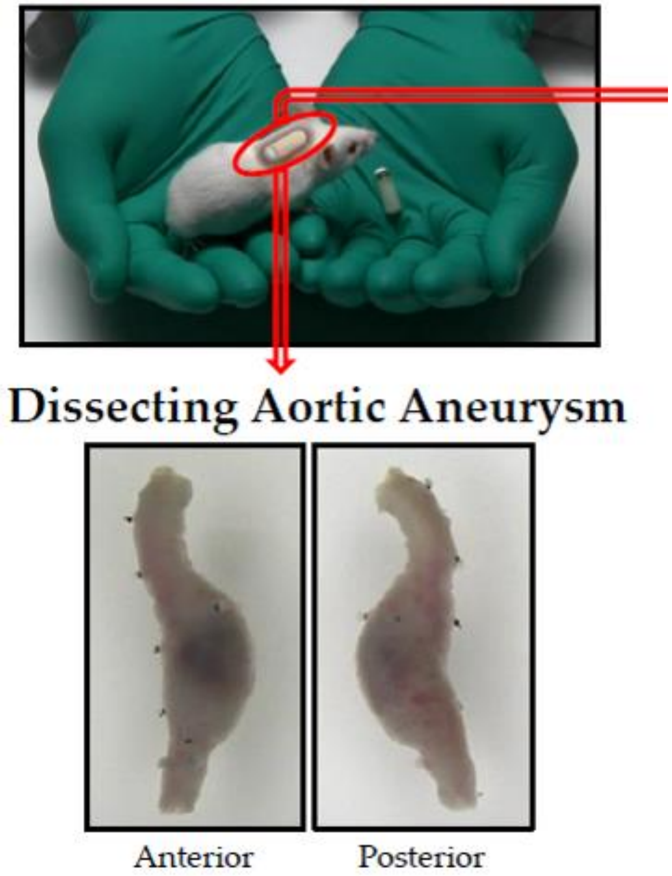

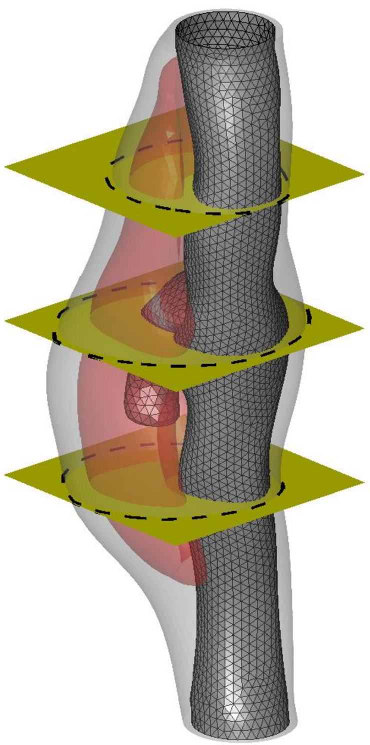

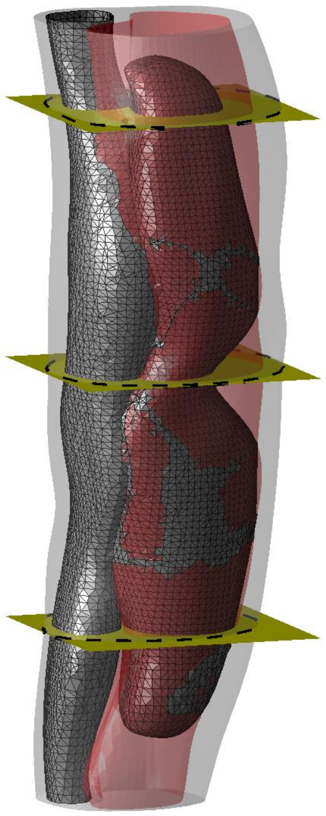

Cross sectional results

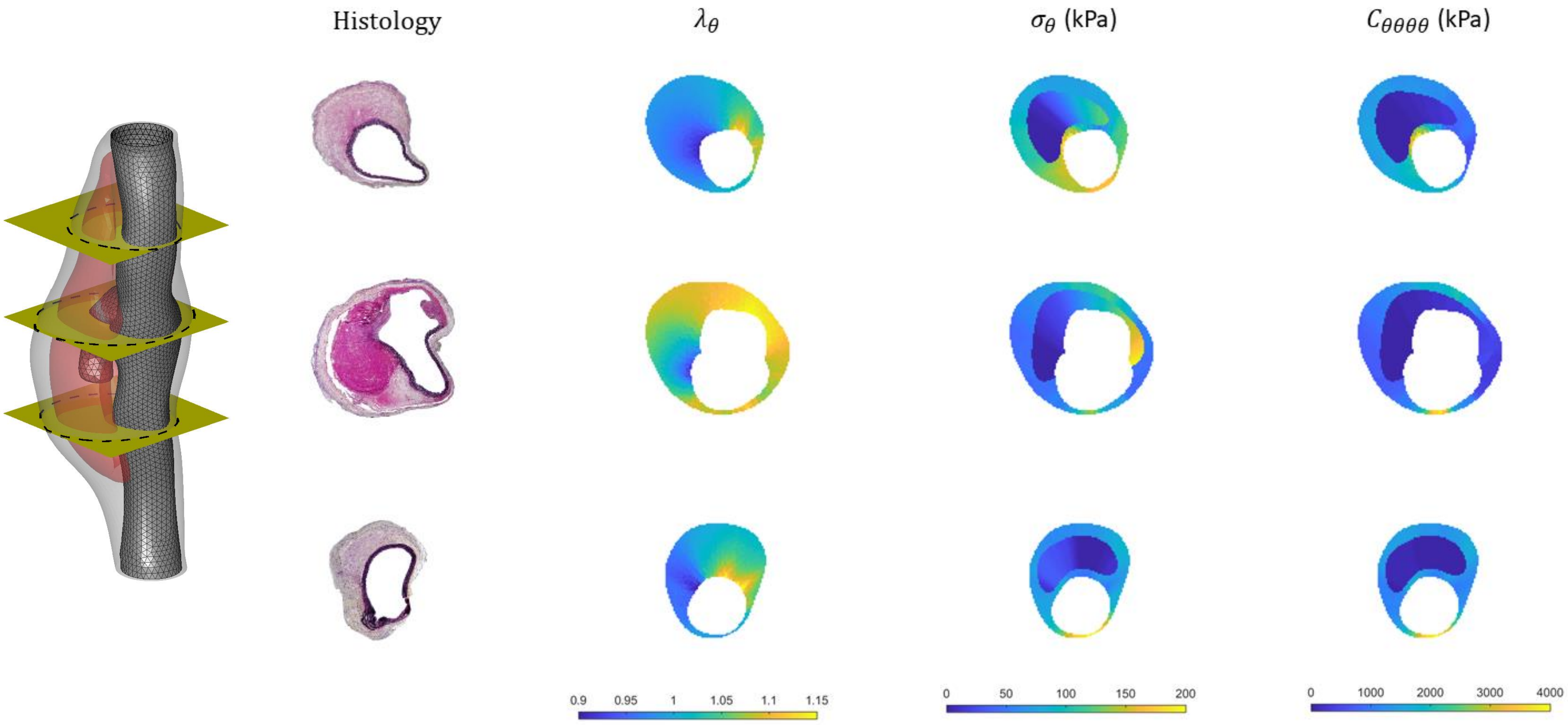

avril@emse.fr

MINES Saint-Étienne

SUMMARY

- ATAA at higher “biomechanical” risk have an increased stiffness and a disturbed flow with reduced maximum TAWSS

- Our future work will focus on idiopathic ATAA and try to understand better what are the main mechanobiological triggers for the overstiffening.

- Need further insight into the relationships between local mechanical properties and protein expression.

avril@emse.fr

Computational Mechanobiology: the holy grail?

"The success of reductionist and molecular approaches in modern medical science has led to an explosion of information, but progress in integrating information has lagged… Mathematical models provide a rational approach for integrating this ocean of data, as well as providing deep insight into biological processes."

1998 BECON Report

avril@emse.fr

Towards computational mechanobiology

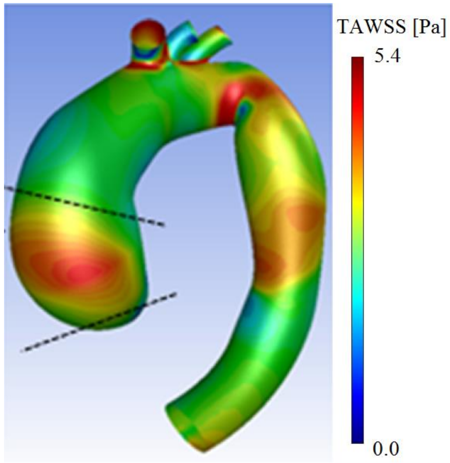

Growth and remodeling of a two–layer patient–specific human ATAAs due to elastin loss

Small growth parameter

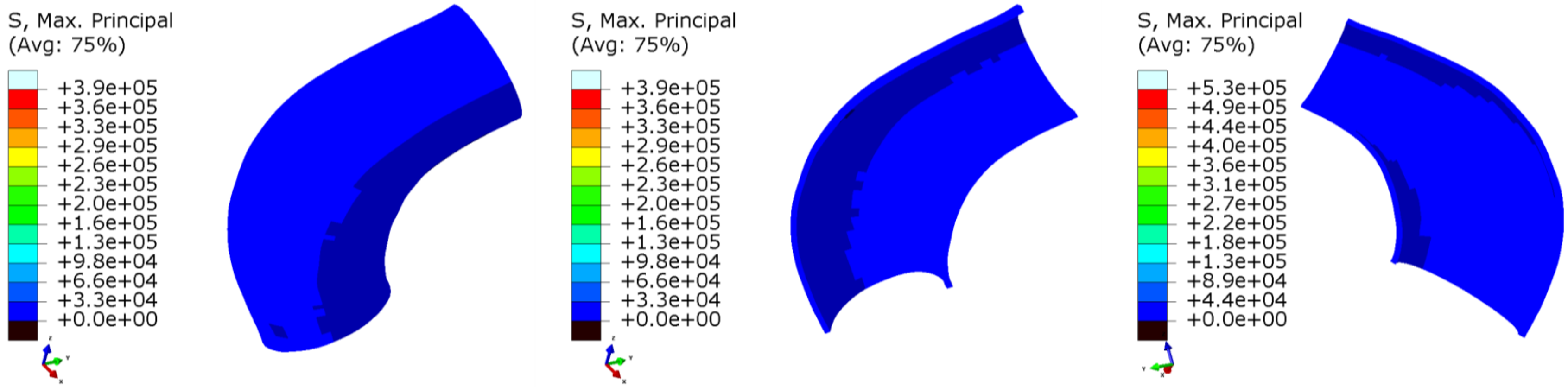

Maximum Principal stress

Mousavi et al, BMMB 2019

Future directions

Monitoring cell vitality

Digital TWIN

NEW PARADIGM:

PREVENTIVE MEDICINE

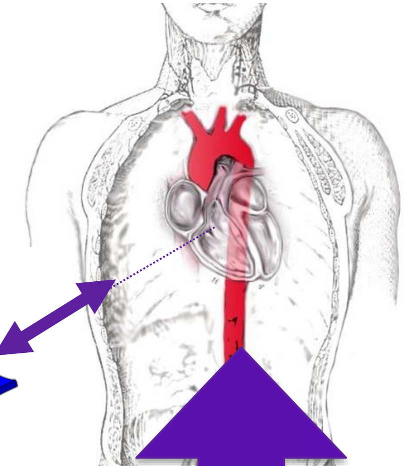

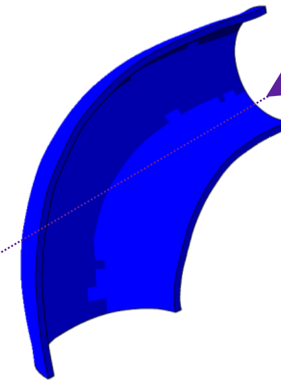

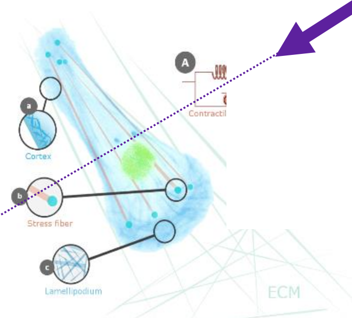

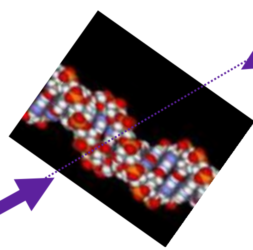

Prevention

Inserm
Institut national de la santé et de la recherche médicale

UNIVERSITÉ DE LYON

SAINBIOSE
SAnté INgénierie BIOlogie Saint-Etienne
U1059 • INSERM • SAINT-ETIENNE

MINES Saint-Étienne
Une école de l'IMT

erc
European Research Council

Assessing cardiovascular health and its evolution

Computational mechanics in the OR for vascular surgery?

www.predisurge.com

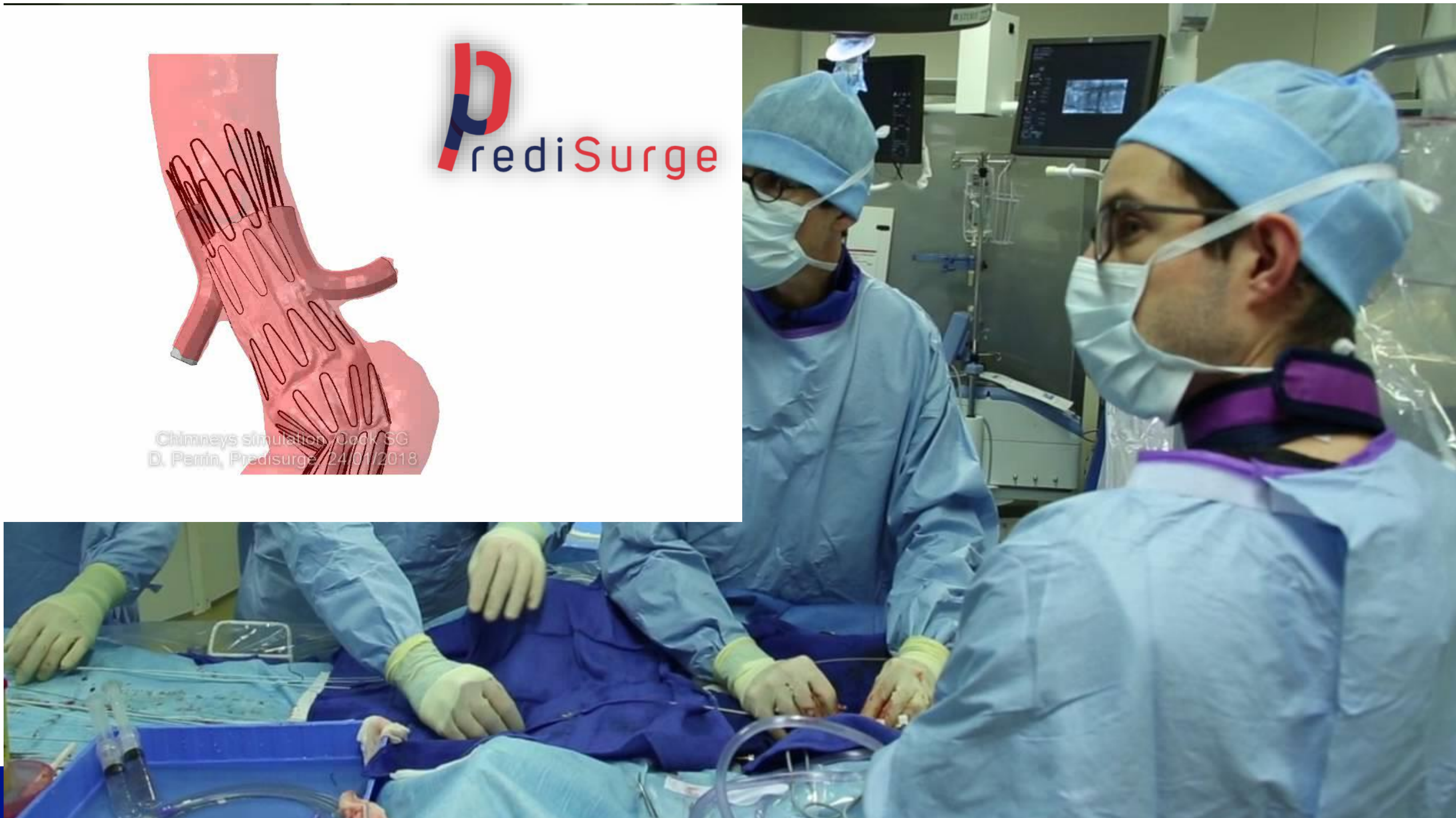

Acknowledgements

- Olfa Trabelsi
- Aaron Romo
- Jin Kim
- Pierre Badel
- Frances Davis
- Victor Acosta
- Jamal Mousavi
- Solmaz Farzeneh
- Francesca Condemi
- Cristina Cavinato
- Jérôme Molimard
- Baptiste Pierrat
- Joan Laubrie
- Claudie Petit

- Ambroise Duprey
- Jean-Pierre Favre
- Jean-Noël Albertini
- Salvatore Campisi
- Magalie Viallon
- Pierre Croisille

- Chiara Bellini
- Matthew Bersi
- Jay Humphrey
- Katia Genovese

Funding:
ERC-2014-CoG BIOLOCHANICS